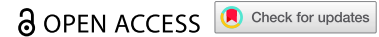









RESEARCH PAPER



Circulating androgen regulation by androgen-catabolizing gut bacteria in male mouse gut

Tsun-Hsien Hsiao ^a, Chia-Hong Chou^b, Yi-Lung Chen ^c, Po-Hsiang Wang ^{d,e}, Guo-Jie Brandon-Mong ^a, Tzong-Huei Lee^f, Tien-Yu Wu^a, Po-Ting Li^b, Chen-Wei Li^a, Yi-Li Lai^g, Yu-Lin Tseng^b, Chao-Jen Shih ^g, Po-Hao Chen^c, Mei-Jou Chen ^{b,h}, and Yin-Ru Chiang ^{a,i}

^aBiodiversity Research Center, Academia Sinica, Taipei, Taiwan; ^bDepartment of Obstetrics and Gynecology, National Taiwan University Hospital and College of Medicine, National Taiwan University, Taipei, Taiwan; ^cDepartment of Microbiology, Soochow University, Taipei, Taiwan; ^dGraduate Institute of Environmental Engineering, National Central University, Taoyuan City, Taiwan; ^eEarth-Life Science Institute (ELSI), Tokyo Institute of Technology, Tokyo, Japan; ^fInstitute of Fisheries Science, National Taiwan University, Taipei, Taiwan; ^gBioresource Collection and Research Center, Food Industry Research and Development Institute, Hsinchu, Taiwan; ^hLivia Shan-Yu Wan Chair Professor of Obstetrics and Gynecology, National Taiwan University, Taipei, Taiwan; ⁱDepartment of Agricultural Chemistry, National Taiwan University, Taipei, Taiwan

ABSTRACT

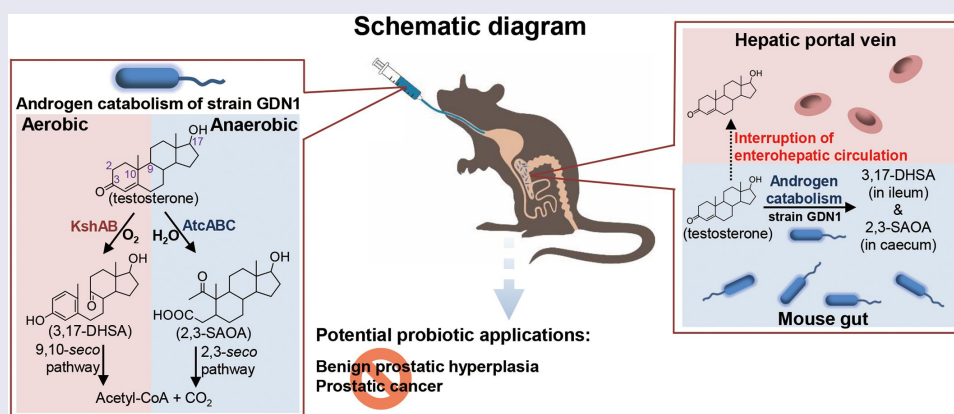
Abnormally high circulating androgen levels have been considered a causative factor for benign prostatic hypertrophy and prostate cancer in men. Recent animal studies on gut microbiome suggested that gut bacteria are involved in sex steroid metabolism; however, the underlying mechanisms and bacterial taxa remain elusive. Denitrifying betaproteobacteria *Thauera* spp. are metabolically versatile and often distributed in the animal gut. *Thauera* sp. strain GDN1 is an unusual betaproteobacterium capable of catabolizing androgen under both aerobic and anaerobic conditions. We administered C57BL/6 mice (aged 7 weeks) with strain GDN1 through oral gavage. The strain GDN1 administration caused a minor increase in the relative abundance of *Thauera* ($\leq 0.1\%$); however, it has profound effects on the host physiology and gut bacterial community. The results of our ELISA assay and metabolite profile analysis indicated an approximately 50% reduction in serum androgen levels in the strain GDN1-administered male mice. Moreover, androgenic ring-cleaved metabolites were detected in the fecal extracts of the strain GDN1-administered mice. Furthermore, our RT-qPCR results revealed the expression of the androgen catabolism genes in the gut of the strain GDN1-administered mice. We found that the administered strain GDN1 regulated mouse serum androgen levels, possibly because it blocked androgen recycling through enterohepatic circulation. This study discovered that sex steroids serve as a carbon source of gut bacteria; moreover, host circulating androgen levels may be regulated by androgen-catabolizing gut bacteria. Our data thus indicate the possible applicability of androgen-catabolic gut bacteria as potent probiotics in alternative therapy of hyperandrogenism.

ARTICLE HISTORY


Received 24 July 2022
Revised 26 October 2022
Accepted 15 February 2023

KEYWORDS

Androgen; gut microbe; hyperandrogenism; mouse; sex steroids; testosterone catabolism; *thauera*



CONTACT Mei-Jou Chen  mjchen04@ntu.edu.tw  Department of Obstetrics and Gynecology, National Taiwan University Hospital and College of Medicine, National Taiwan University, Taipei 106, Taiwan; Yin-Ru Chiang  yinru915@gate.sinica.edu.tw  Biodiversity Research Center, Academia Sinica, 128 Academia Road Sec. 2, Nankang, Taipei 115, Taiwan

 Supplemental data for this article can be accessed online at <https://doi.org/10.1080/19490976.2023.2183685>

© 2023 The Author(s). Published with license by Taylor & Francis Group, LLC.

This is an Open Access article distributed under the terms of the Creative Commons Attribution License (<http://creativecommons.org/licenses/by/4.0/>), which permits unrestricted use, distribution, and reproduction in any medium, provided the original work is properly cited.

Introduction

Sex steroids, such as androgens, modulate vertebrate physiology, development, reproduction, and behavior¹. Vital androgens include testosterone, dihydrotestosterone (DHT), and androstenedione. Androgens have been considered a critical mediator of androgenetic alopecia², benign prostatic hypertrophy^{3,4}, and prostate cancer⁵ in men. An excess of circulating androgens can cause polycystic ovary syndrome in women⁶.

In mammals, sex steroids are excreted through either feces or urine; for instance, male mice excrete significantly more androgens through feces (approximately 60%) than female mice (<50%)⁷. Steroids are recycled between the liver and the gut through enterohepatic circulation. Cholesterol and bile acids may be recycled more than 10 times before being excreted through feces^{8,9}; the reabsorption of these steroids occurs mainly in human small intestine¹⁰ as well as rodent small intestine and cecum^{11,12}. By contrast, little is known regarding the metabolic fate and flux of sex steroids in the mammalian gut. Current knowledge indicates that androgens undergo glucuronidation in the liver and are then delivered into the gut. The conjugated androgens become less susceptible to reabsorption and are eventually excreted through feces¹³. Recent studies have also reported that gut microbes can mediate deglucuronidation, which increases free androgen levels in the mouse cecum and human colon⁴. The deconjugated androgens, mainly testosterone and DHT, are present in the bacteria-rich colon of young men at concentrations much higher than those in the serum⁴. Most gut androgens (approximately 80%) are reabsorbed into the blood through enterohepatic circulation^{14,15}.

Sex steroids may be involved in bidirectional metabolic interactions between bacteria and their vertebrate hosts^{16,17}; however, the underlying mechanisms and bacterial taxa remain largely unknown. Understanding these underlying mechanisms warrants the examination of host – microbe interactions, particularly the examination of the microbial metabolic contributions to the host metabolome, at the molecular level^{18–22}. There is some evidence that sex may influence the diversity, composition, and function of gut

bacterial microbiota²², although the results are inconsistent. The contribution of the gut microbiota to the host steroid metabolome and to the host endocrine system might be the key in understanding the role of sex as a biological variable under both healthy and disease conditions. For instance, a recent gut microbiome study revealed that some gut microbes (e.g., *Ruminococcus gnavus*) contribute to endocrine resistance in castration-resistant prostate cancer through the transformation of pregnenolone (precursor of steroid hormones) to androgens⁵, increasing circulating androgen levels through enterohepatic circulation and thus enhancing prostate cancer growth in the host.

The bacterial catabolism of sex steroids has been characterized at the molecular level [see²³ for a recent review]. Aerobic androgen catabolism through the steroid 9,10-*seco* pathway has been well characterized^{24–26}; it includes 3,17-dihydroxy-9,10-*seco*-androsta-1,3,5(10)-triene-9-one (3,17-DHSA)²⁷ and the 3-ketosteroid 9 α -hydroxylase gene *kshAB*²⁸ as characteristic androgen metabolite and degradation genes, respectively. By using several denitrifying proteobacteria as the model organisms, we previously established an anaerobic degradation pathway (the steroid 2,3-*seco* pathway) for androgens; moreover, the 17 β -hydroxy-1-oxo-2,3-*seco*-androstan-3-oic acid (abbreviated as 2,3--SAOA)²⁹ and *atcABC* encoding the 1-testosterone hydratase/dehydrogenase³⁰ were identified as the characteristic androgen metabolite and degradation genes for this anaerobic pathway, respectively. However, androgen catabolism has not been reported in the animal gut. Facultative anaerobes *Thauera* spp. are widely distributed in O₂-limited environments, such as in the estuarine sediment³¹ and denitrifying sludge³⁰ as well as in chicken³², pig³², duck³³, and human^{34–36} intestines. Thus far, at least two *Thauera* species have been identified as anaerobic androgen degraders^{30,31}.

In this study, we used *Thauera* sp. strain GDN1³¹ (referred as strain GDN1 hereafter) as the model microorganism because (i) strain GDN1 can utilize major androgens as the sole carbon sources and as electron donors under both aerobic and anaerobic (denitrifying) conditions, (ii) strain GDN1 can efficiently degrade testosterone in environmental conditions (37°C and pH

6.0) resembling the mammalian gut, and (iii) *Thauera* spp. are often detected in the animal gut, but their functions in their hosts remain unknown. We performed tiered functional genomic analyses to identify the characteristic metabolites and degradation genes of strain GDN1 involved in aerobic and anaerobic androgen catabolism. Subsequently, we administered mice with strain GDN1 through oral gavage and monitored its androgen-catabolic activities in mouse intestines. We also collected fecal samples from mice with different treatments and examined how the gut bacterial communities of mice varied across different treatments. Finally, the changes in host circulating androgen levels and profiles were determined using enzyme-linked immunosorbent assay kit (ELISA) and ultraperformance liquid chromatography – high-resolution mass spectrometry (UPLC – HRMS), respectively.

Results

Physiological and multi-omics analyses for strain GDN1 growth and androgen catabolism

The mammalian gut is an O₂-limited environment, but often with a low abundance of facultative anaerobic and microaerobic microorganisms³⁷. Thus far, only four bacterial strains, namely *Steroidobacter denitrificans* DSMZ18526³⁸, *Sterolibacterium denitrificans* DSMZ13999³⁹, *Thauera terpenica* 58Eu³⁰, and strain GDN1³¹, are reportedly able to anaerobically catabolize testosterone at 25°C–28°C and neutral pH (6.5–7.5). First, we characterized the physiology of these facultative anaerobes and evaluated their androgen-catabolic potentials in the mammalian gut. We anaerobically grew these bacteria with testosterone at 37°C and pH 6.0, and only strain GDN1 apparently degraded testosterone within 2 days (Figure 1A). We observed that substrate consumption accompanied a decrease in androgenic activity as well as nitrate reduction with time. Moreover, we detected temporal production of the androgenic metabolite 2,3-SAOA in the denitrifying bacterial culture (Figure 1B; left panel). However, strain GDN1 could not degrade testosterone anaerobically in the chemically defined medium without exogenous nitrate (Figure 1B; right panel), indicating the incapability of androgen catabolism under

fermentative conditions. We also observed aerobic testosterone catabolism and decreased androgenic activity in a phosphate-buffered minimal medium, with 3,17-DHSA being the characteristic androgen metabolite (Figure 1C). These ring-cleaved metabolites are specific for androgen catabolism^{27,29} and exhibit negligible androgenic activity³⁹. These androgenic metabolites are thus suitable molecular markers for monitoring bacterial androgen catabolism in the mammalian gut. In addition to testosterone, strain GDN1 was able to degrade other major androgens including DHT and androstadienedione (1 mM for each) in a denitrifying minimal medium at 37°C and pH 6.0 (Figure 2A). By contrast, strain GDN1 could not degrade other sex steroids including progesterone and 17β-estradiol (Figure 2B). The physiological test results thus support strain GDN1 growth in the mammalian gut and suggest its metabolic specificity for androgen metabolism.

We then elucidated the biochemical mechanisms underlying androgen catabolism in strain GDN1 and identified the potential biomarkers of androgen catabolism through genomic approaches. We could identify gene clusters specific for aerobic and anaerobic androgen catabolism (Figure 3A; see detailed genomic analysis in SI Results). Of these, the gene products (namely the bifunctional 1-testosterone hydratase/dehydrogenase) of *atcABC* (CKCBHOJB_02409–2411; Dataset S1) mediate O₂-independent androgenic A-ring activation by adding a hydroxyl group at C-1 of testosterone³⁰, with 2,3-SAOA as the downstream product. By contrast, the 3-ketosteroid 9α-hydroxylase gene (*kshAB*; CKCBHOJB_02264 and 02279; Dataset S1) is responsible for the O₂-dependent cleavage of the androgen B-ring²⁸, with 3,17-DHSA as the product.

To identify the inducers of these androgen catabolism genes, we incubated strain GDN1 with acetate (10 mM) or testosterone (2 mM) under aerobic and anaerobic conditions. The transcriptomes of strain GDN1 cells were then sequenced on an Illumina-based platform. We detected the distinguishable expression of *atcA* and *kshA* in the testosterone-grown cells, regardless of the oxygen conditions [Figures. 3B (right panel); see detailed transcriptome analysis in SI Results]. However, we observed low expression of these androgen

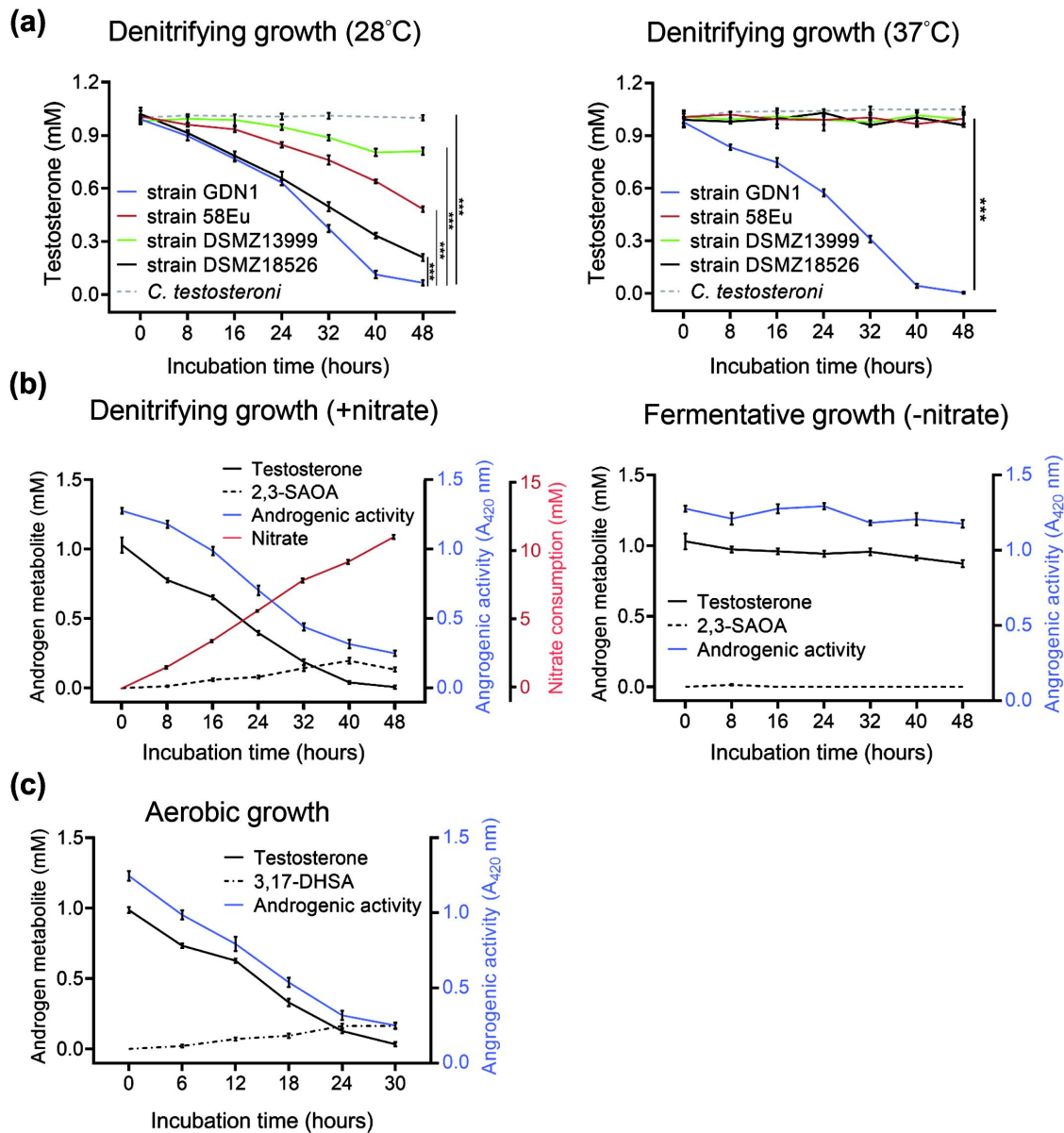


Figure 1. Physiological tests of the testosterone-grown strain GDN1. (a) denitrifying growth of several androgen-catabolic anaerobes with testosterone at 28°C and 37°C. The anaerobic androgen utilization of *comamonas testosteroni* strain TA441, a betaproteobacterium capable of aerobic androgen catabolism, was also tested for a comparison. (b) Nitrate is required for anaerobic androgen catabolism of strain GDN1. androgenic activity in bacterial cultures was determined using a yeast androgen bioassay. (c) aerobic androgen catabolism of strain GDN1. results are the representative of three individual experiments. all data are shown as means \pm SEM. statistical results were calculated using welch's *t*-test; *** p <0.001.

catabolism genes in the acetate-grown strain GDN1 cells (Figures. 3B; left panel). The expression levels of *atcA* and *kshA* in the same conditions were also confirmed using reverse transcription (RT)-quantitative polymerase chain reaction (qPCR) analysis (Fig. S1). Our multi-omics data thus indicated that (i) strain GDN1 can aerobically and anaerobically catabolize androgen through the established 9,10-*seco*⁴⁰ and 2,3-*seco*²⁹ pathways, respectively, and (ii) the gene expression of the

androgen catabolism genes *atcABC* (for anaerobic catabolism) and *kshAB* (for aerobic catabolism) is induced by the substrate (androgen). The subunits AtcA and KshA contain molybdopterin³⁰ and a mononuclear iron center⁴¹, respectively – which are essential cofactors for their catalytic activities. Therefore, we believe that *atcA* and *kshA* are suitable biomarkers for monitoring the anaerobic and aerobic androgen catabolism, respectively, in the animal gut.

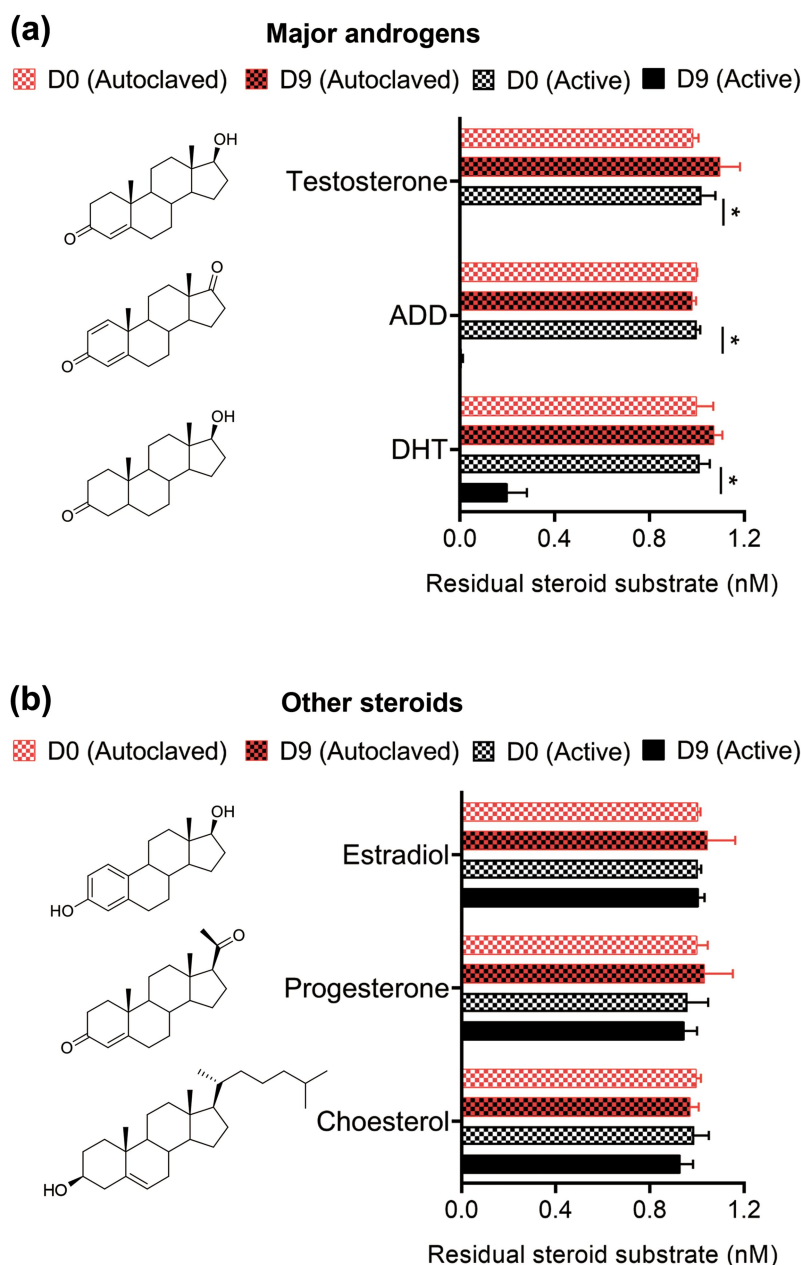


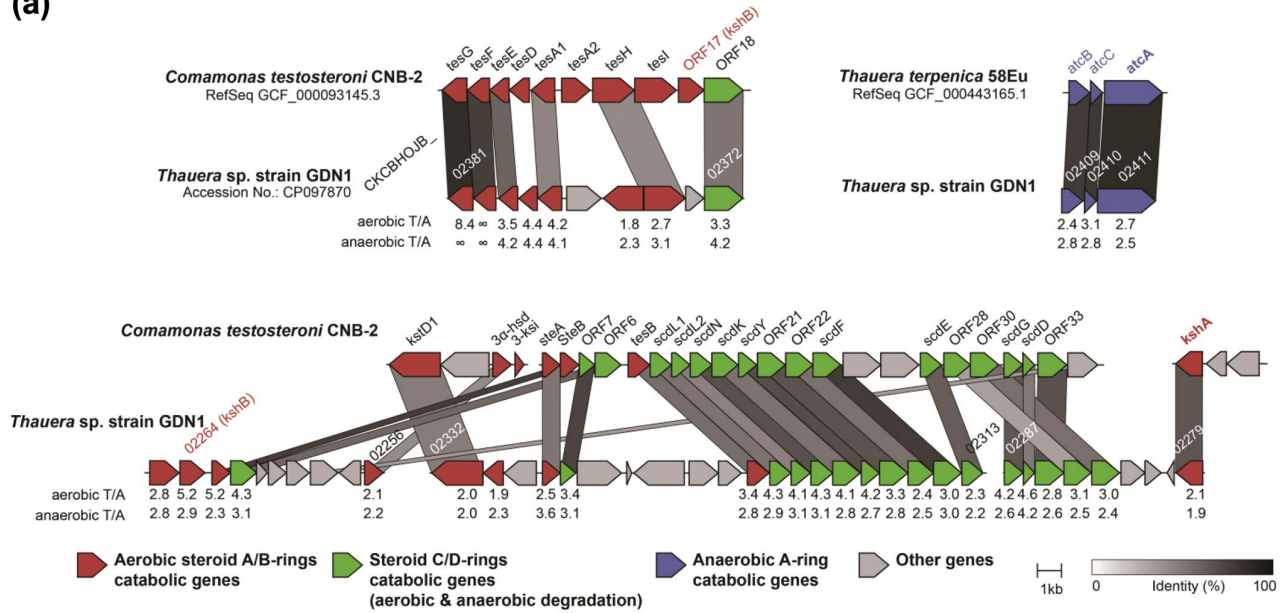
Figure 2. Steroid utilization patterns of strain GDN1. The bacterial cultures of autoclaved strain GDN1 cells were used as negative controls. androgen metabolites were detected and quantified through UPLC – ESI–HRMS. results are the representative of three individual experiments. all data are shown as mean \pm SEM. statistical results were calculated using unpaired nonparametric *t*-test; **p*<0.05. abbreviations: androstadienedione, ADD; dihydrotestosterone, DHT.

Administration of strain GDN1 to mice through oral gavage and resulting changes in host serum androgen levels

Strain GDN1, a facultative anaerobic bacterium, was aerobically grown in tryptone soy broth, and the cells were harvested in the log phase [optical density at 600 nm (OD_{600}) = 0.5–0.7]. These cells were resuspended in a basal mineral medium and stored at 4°C (within 5 days) before use. The

resting strain GDN1 suspension (200 μ L; containing approximately 5×10^8 colony-forming units) was administered into mouse gut through oral gavage twice per week. C57BL/6J mice (aged 7 weeks) were used as the model host. All the included mice were treated with exogenous nitrate (an electron acceptor for anaerobic androgen catabolism of strain GDN1; supplemented in drinking water at a final concentration of 2 mM). The mice

(a)



(b)

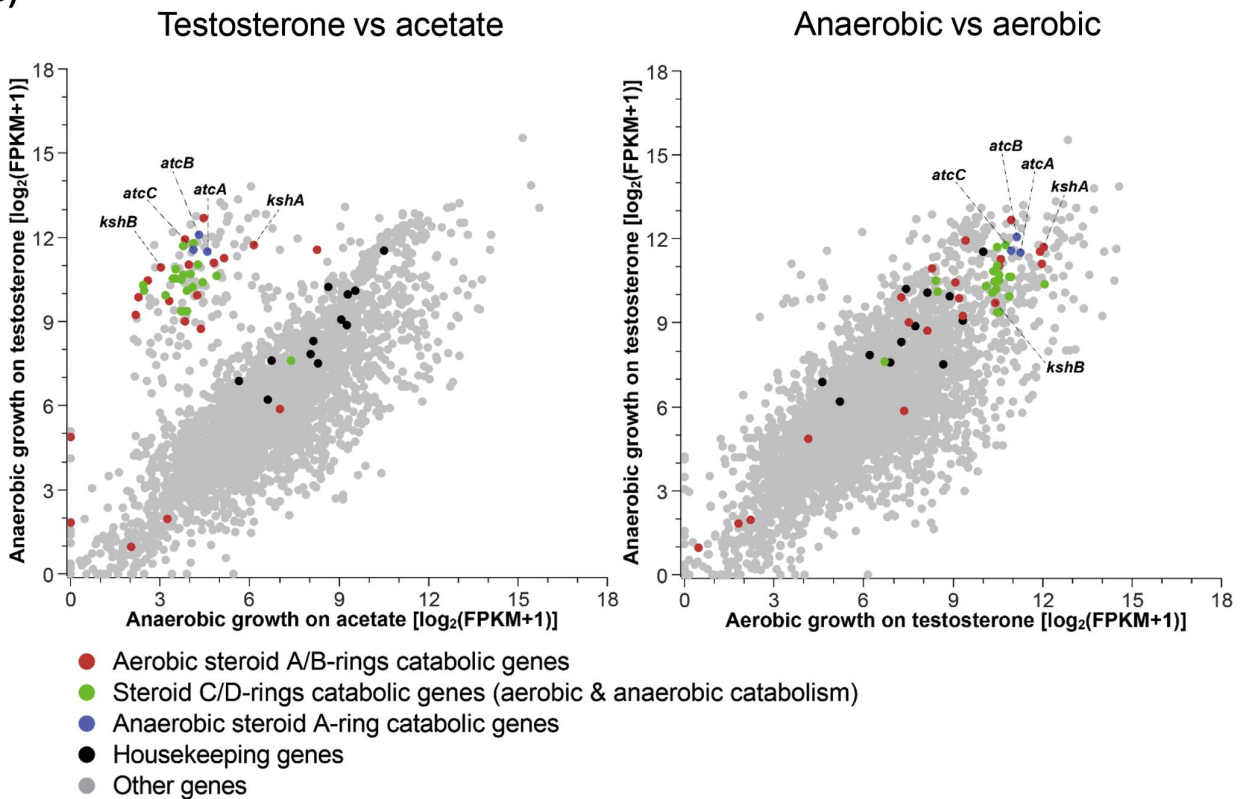


Figure 3. Identification and expression of androgen catabolism genes of strain GDN1. (a) gene synteny of androgen catabolism in the strain GDN1 chromosome (accession no.: CP097870). strain GDN1 uses the gene products of *atcABC* and *kshAB* to catabolize androgen anaerobically and aerobically, respectively. ORFs homologous between different bacterial strains are connected by columns with different gray scaling, according to the similarities of deduced amino acid sequences. numbers below individual ORFs of strain GDN1 indicate the gene expression ratios, which are derived from the logarithmic transformation of differential gene expression levels of strain GDN1 grown with acetate (abbreviation: A) or testosterone (abbreviation: T) under aerobic and anaerobic (denitrifying) conditions. Androgen catabolism genes are named according to those characterized in two androgen-degrading bacteria: *Comamonas testosteroni* strain CNB-2 (aerobic androgen degrader) and *thauera terpenica* 58eu (anaerobic androgen degrader). synteny analysis was conducted using clinker v0.023 (<https://github.com/gamcil/clinker>). (b) global gene expression profiles (RNA-Seq) of strain GDN1 grown under different conditions [anaerobic growth with testosterone or acetate (left panel); anaerobic or aerobic growth with testosterone (right panel)]. each spot represents a gene. gene expression levels were estimated using fragments per kilobase of transcript per million mapped reads (FPKM).

were treated as follows: (i) female mice administered with nitrate (2 mM in drinking water) and with (strain GDN1 treatment; $n = 8$) or without (vehicle treatment; $n = 8$) strain GDN1 administration and (ii) male mice administered with nitrate and with (strain GDN1 treatment; $n = 13$) or without (vehicle treatment; $n = 14$) strain GDN1 administration (Figure 4A). During the continual strain GDN1 administration period, we did not observe considerable weight loss or appetite loss among our mice (Fig. S2).

We then used ELISA and UPLC – HRMS to determine the androgen levels and profiles in the mouse sera. After 25 days of continual administration of strain GDN1, we observed a considerable decrease in serum androgen levels (expressed as testosterone equivalents; see detailed information in the Materials and Methods) in the strain GDN1-

administered male mice (Figure 4B). The ELISA results indicated that serum androgen levels (testosterone equivalents) were considerably lower in the strain GDN1-administered male mice (4.38 ± 0.27 ng/mL) than in the vehicle-administered mice (9.33 ± 0.95 ng/mL). Notably, serum androgen levels in our healthy male mice (in the vehicle group) demonstrated extreme deviation (in the range of 4–15 ng/mL), and the administration of strain GDN1 to the male mouse gut considerably reduced this deviation (in the range of 3–6 ng/mL). By contrast, we did not observe a considerable decrease in serum androgen levels in the strain GDN1-administered female mice (Figure 4B). Our data thus indicate that androgen-mediated strain GDN1–mouse interactions are gender-dependent. The serum androgen profile analysis through UPLC – HRMS indicated that testosterone

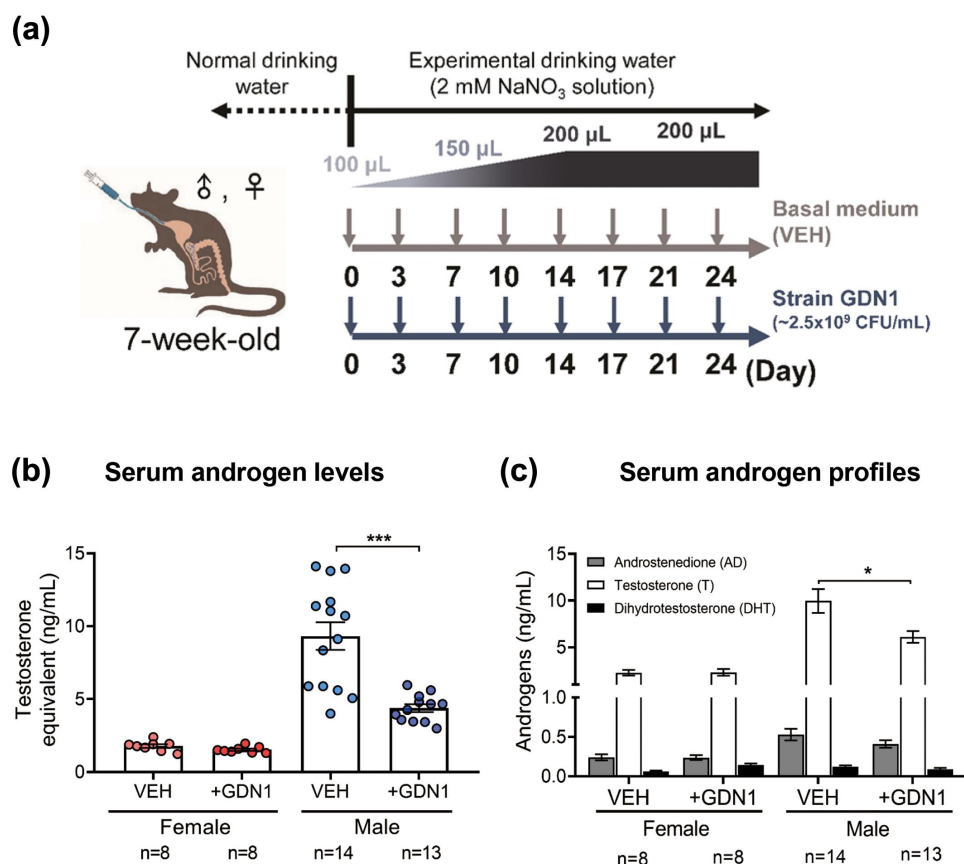


Figure 4. Administration of androgen-catabolic *Thauera* sp. strain GDN1 into mouse gut through oral gavage can regulate host circulating androgen levels. (a) Working flow of the administration of mice with strain GDN1 through oral gavage. Nitrate (2 mM) was supplemented in the drinking water during the period of continuous administration. (b) Administration of male mice with strain GDN1 through oral gavage for 25 days reduces serum testosterone levels considerably. (c) Strain GDN1 administration does not affect the serum androgen metabolite profiles of male and female mice considerably. Testosterone is the most dominant serum androgen (>90%, w/w) in all the included mice. Results are representative of three individual experiments. Statistical results were calculated with unpaired nonparametric *t*-test; * $p < 0.05$, *** $p < 0.001$. All data are shown as means \pm SEM of 8–14 mouse individuals.

(9.96 ± 1.27 ng/mL), androstenedione (0.53 ± 0.07 ng/mL), and DHT (0.12 ± 0.02 ng/mL) were the major androgens in the male vehicle-administered mice. Of these, only testosterone (6.11 ± 0.63 ng/mL after strain GDN1 treatment) considerably decreased in the strain GDN1-administered male mice (Figure 4C). By contrast, we did not observe apparent differences in the serum androgen profiles between the female mice administered with vehicle (2.28 ± 0.29 ng/mL testosterone in the serum) and strain GDN1 (2.31 ± 0.36 ng/mL testosterone in the serum). In contrast to serum testosterone levels, serum estradiol levels did not significantly change after strain GDN1 administration compared with that after vehicle administration for both the male and female mice (Fig. S3).

The expression of androgen catabolism genes in mouse gut

The changes in the serum androgen levels of the strain GDN1-administered male mice suggested that strain GDN1 can regulate circulating androgen levels in male mice. To elucidate the mechanisms underlying the gut bacteria – host interactions, we determined the androgen-catabolic activity of strain GDN1 in the mouse gut. After 25 days of administration with strain GDN1, we sacrificed the mice and extracted the bacterial DNA from the mouse gastrointestinal (GI) contents to determine the abundance of *Thauera* spp. in the ileum, cecum, and colon through qPCR (Figure 5). The results of qPCR using *Thauera*-specific primers suggested that *Thauera* spp. mainly inhabited the cecum [$(3.9 \pm 1.5) \times 10^6$ copies/g of GI content] of the strain GDN1-administered male mice (Figure 5A). By contrast, *Thauera* spp. mainly inhabited the colon [$(0.9 \pm 0.7) \times 10^6$ copies/g of GI content] of the vehicle-administered mice. Moreover, we extracted RNA from the mouse GI contents of the ileum, cecum, and colon and then performed RT-qPCR to examine the relative expression of strain GDN1-specific 16S rRNA and androgen catabolism genes by using the $2^{-\Delta\Delta Ct}$ method⁴². Among all vehicle- and GDN1-administered mouse GI contents, the strain GDN1 16S rRNA was expressed at the highest level in the cecum of the GDN1-administered

male mice (375-fold higher than that in the vehicle-administered male mouse ileum; Figure 5B). By contrast, strain GDN1-specific 16S rRNA was not considerably expressed in the vehicle-administered mouse gut. These data indicated the occurrence of strain GDN1 mainly in the mouse cecum. To confirm the viability of strain GDN1 in the mouse gut, we incubated fecal samples from the strain GDN1- and vehicle-administered mice (25 days after the first administration) with testosterone (1 mM) under denitrifying conditions. After 3 days of anaerobic incubation at 37°C and pH 6.0, apparent testosterone consumption was observed only in the denitrifying culture spiked with feces from the strain GDN1-administered mice (Figure 6). These results indicate that strain GDN1 has a high survival rate in the mouse gut.

We then applied RT-qPCR to investigate the expression of the androgen catabolism genes in the mouse gut. We determined *atcA* expression in the mouse gut, with the highest *atcA* expression in the cecum of the strain GDN1-administered male mice (7.92-fold higher than that in vehicle-administered male mouse ileum; Figure 5C). Notably, we also detected the expression of *kshA* in the mouse gut; *kshA* expression in the ileum of the strain GDN1-administered male mice was 294-fold higher than that in the ileum of the vehicle-administered mice (Figure 5D).

Impact of strain GDN1 administration on mouse gut microbiota

We next sought to examine how the gut bacterial communities varied across different mouse treatments. After normalizing all samples to 48,558 reads, 993,457 amplicon sequence variants (ASVs) were generated, which belong to 280 bacterial genera, 118 families, and 12 phyla. The non-metric multidimensional scaling (NMDS) ordination indicated that the gut bacterial communities of male mice did not cluster by the strain GDN1 administration (Figure 7A; right panel), although permutational multivariate analysis of variance (PERMANOVA) based on Bray-Curtis dissimilarity matrix indicated a difference in the clustering (F-value = 2.451, global $R^2 = 0.100$, p value = 0.026). In contrast, among female mice, the gut bacterial community structure of the strain GDN1-

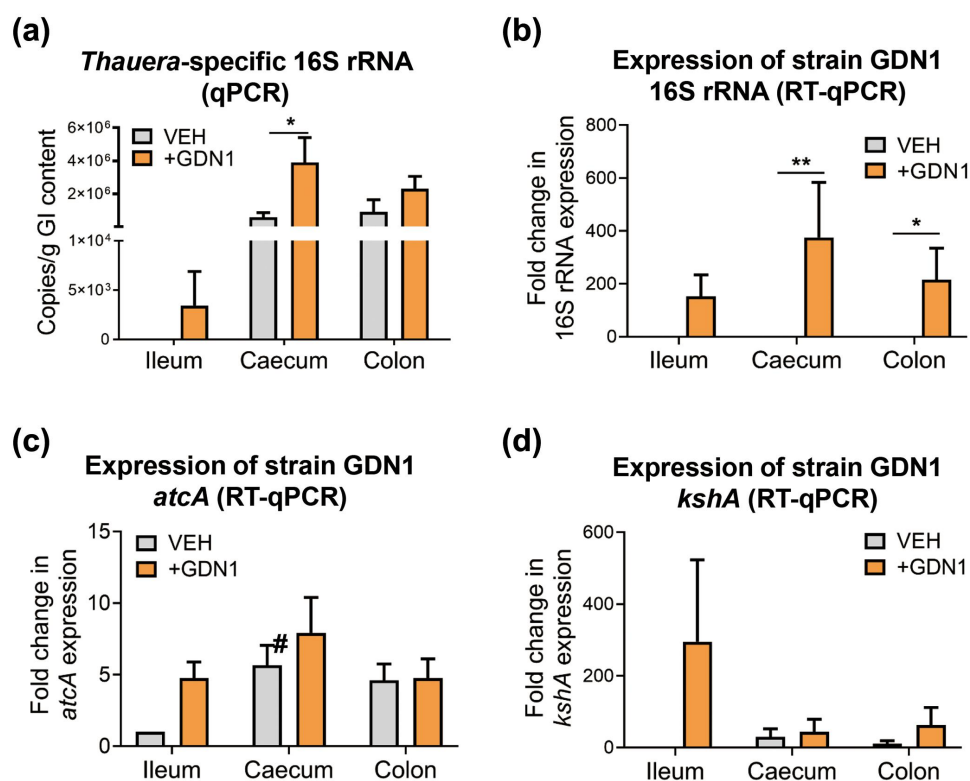


Figure 5. Determination of the abundance and relative expression of *Thauera* genes in the mouse GI tract. (a) determination of *Thauera* 16S rRNA copy number in the mouse GI contents using qPCR. all data are shown as means \pm SEM of 5 randomly selected male mice. statistical results were computed with unpaired nonparametric *t* test; * p <0.05. (B – D) determination of relative expression of strain GDN1-specific 16S rRNA (b), *atcA* (c), and *kshA* (d) in the mouse GI contents using RT-qPCR. relative change in gene expression was calculated using the $2^{-\Delta\Delta Ct}$ method with the Ct value of universal 16S rRNA of bacteria as the internal control. The expression of individual genes in the vehicle-administered mouse ileum was set as 1. results are representative of three individual experiments. statistical results were calculated with unpaired nonparametric *t*-test; * p <0.05, ** p <0.01. all the data are shown as mean \pm SEM of 5 randomly selected male mice. #, expression of inherent *atcA*-like gene (see appendix S4 for nucleotide sequence).

administered female mice (GF) clustered distinctly from that of the vehicle-administered female mice (VF) as confirmed by PERMANOVA (F-value = 4.085, global $R^2 = 0.157$, p value < 0.001; Figure 7A; left panel). Our data thus indicated a discernible change in the gut bacterial community structure of female mice by the strain GDN1 administration.

Of the 12 identified bacterial phyla, 5 phyla dominated the mouse gut microbiota (average cumulative abundance = 98.5%), namely Firmicutes (synonym Bacillota), Bacteroidetes (synonym Bacteroidota), Verrucomicrobiota, Actinobacteria (synonym Actinobacteriota), and Proteobacteria (synonym Pseudomonadota) (Figure 7B). Among them, Firmicutes (relative abundance = 46.7%) and Bacteroidetes (relative abundance = 42.7%) comprised the most dominant phyla in the mouse gut microbiota; Proteobacteria was the least dominant (relative abundance = 8.5%). Although all test mice

were treated with 2 mM nitrate (supplemented through drinking water), we did not observe an apparent increase in the abundance of denitrifying proteobacteria. We observed an apparent decrease in the abundance of Verrucomicrobiota and Actinobacteria in the gut of strain GDN1-administered female (GF) mice (Figure 7B; left panel). Furthermore, in the gut of female mice, we identified 3 bacterial families within Verrucomicrobiota (e.g., Akkermansiaceae and 2 unclassified families) that are most affected by the strain GDN1 administration (Figure 7C; upper panel). In addition, we observed an apparent decrease in the relative abundance of the family Bifidobacteriaceae (Phylum Actinobacteria) in the GM and GF mice (Figure 7C). In the strain GDN1-administered male mice (GM), we also observed a decrease in the abundance of other families, including Erysipelatoclostridiaceae (Firmicutes),

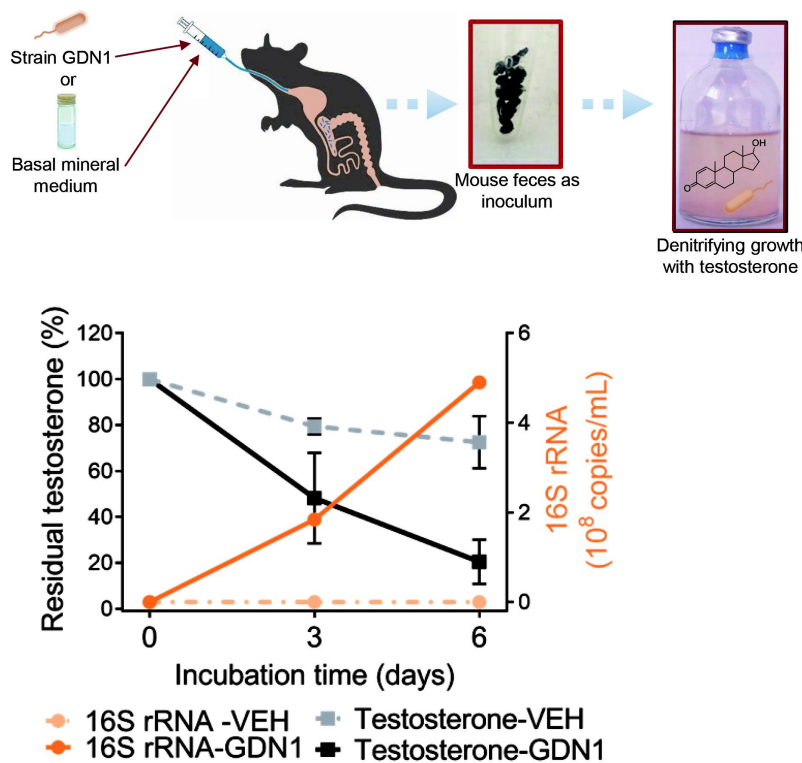


Figure 6. Anaerobic growth of fecal bacteria from the strain GDN1-administered mice (abbreviation: GDN1) or vehicle-administered mice (VEH) mice with testosterone (1 mM; set as 100%) as sole carbon source. After 25 days of continual administration, the fresh mouse feces (approximately 0.1 g) were collected and immediately incubated with testosterone in a denitrifying medium, and the temporal changes in substrate consumption and the copy number of *Thauera* 16S rRNA in bacterial cultures were determined. The residual testosterone concentration was examined using HPLC. The copy number of *Thauera* 16S rRNA was determined through qPCR.

Erysipelotrichaceae (Firmicutes), Staphylococcaceae (Firmicutes), Enterobacteriaceae (Proteobacteria), and Rhodospirillales_uncultured (Proteobacteria). In the GM treatment, the strain GDN1 administration resulted in the increase in the abundance of gut bacteria belonging to Zoogloeaceae (Proteobacteria), Bacteroidales_unclassified (Bacteroidetes), Bacteroidia_unclassified (Bacteroidetes), and Clostridia_unclassified (Firmicutes) (Figure 7C; bottom panel).

In the mice administered with strain GDN1, we observed an increase in the *Thauera* population (Fig. S4). After 3 weeks of the first administration, the relative abundance of *Thauera* reached approximately 0.1% in the gut of both GF and GM mice. By contrast, the relative abundance of *Thauera* remained low (<0.01%) in the gut of the vehicle-administered mice.

We then managed to elucidate potential microbial interactions within individual gut microbial

communities. The SparCC networks were generated and only high-scoring eigenvector centrality nodes (top 30 microbial genera) are shown (Figure 8). In general, the gut microbiota of both male (Figure 8A) and female (Figure 8B) mice administered with strain GDN1 showed fewer positive interactions (represented by red edges) between bacterial genera. In the GF gut microbial community, we identified Anaerovoraceae_unclassified (rank 1), *Colidextribacter* (rank 2), and *Butyricoccus* (rank 3) as the top 3 key microbes (Figure 8A; right panel). In the GM gut microbial community, we identified *Butyricoccus* (rank 1), Oscillospiraceae_uncultured (rank 2), and *Oscillibacter* (rank 3) as the top 3 key microbes (Figure 8B; right panel). Most of the identified key microbes belong to the phylum Firmicutes (Figure 8). *Thauera* was identified as an important microbe (with a high-scoring eigenvector centrality; rank 13) in the

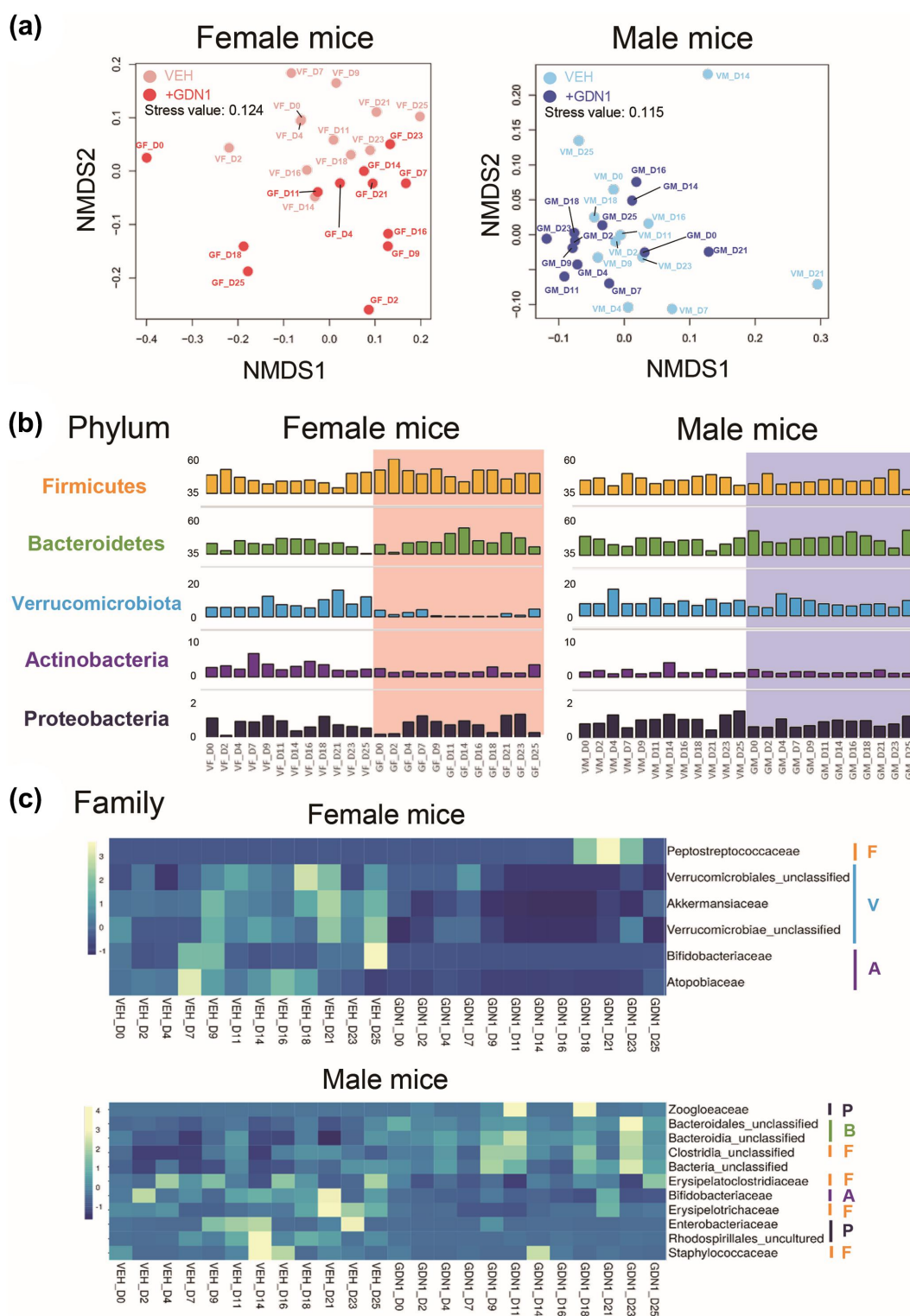


Figure 7. Impact of strain GDN1 administration on mouse gut microbiota. **(a)** Gut bacterial communities across the mouse treatments. NMDS analysis based on Bray-Curtis distance matrix data (genus level) was used to determine the similarities between the gut bacterial communities from different mouse treatments, including the vehicle-administered male mice (VM), strain GDN1-administered male mice (GM), vehicle-administered female mice (VF), and strain GDN1-administered female mice (GF). numbers shown are the days after the first oral administration. **(b)** relative abundances of the most prevalent bacterial phyla (bar length) in the mouse fecal samples. **(c)** relative abundance changes of major bacteria families in the fecal samples from different mouse treatments. Bacterial phyla: ochre, Firmicutes (F); green, Bacteroidetes (B); purple, Actinobacteria (A); light blue, Verrucomicrobiota (V); Dark blue, Proteobacteria (P).

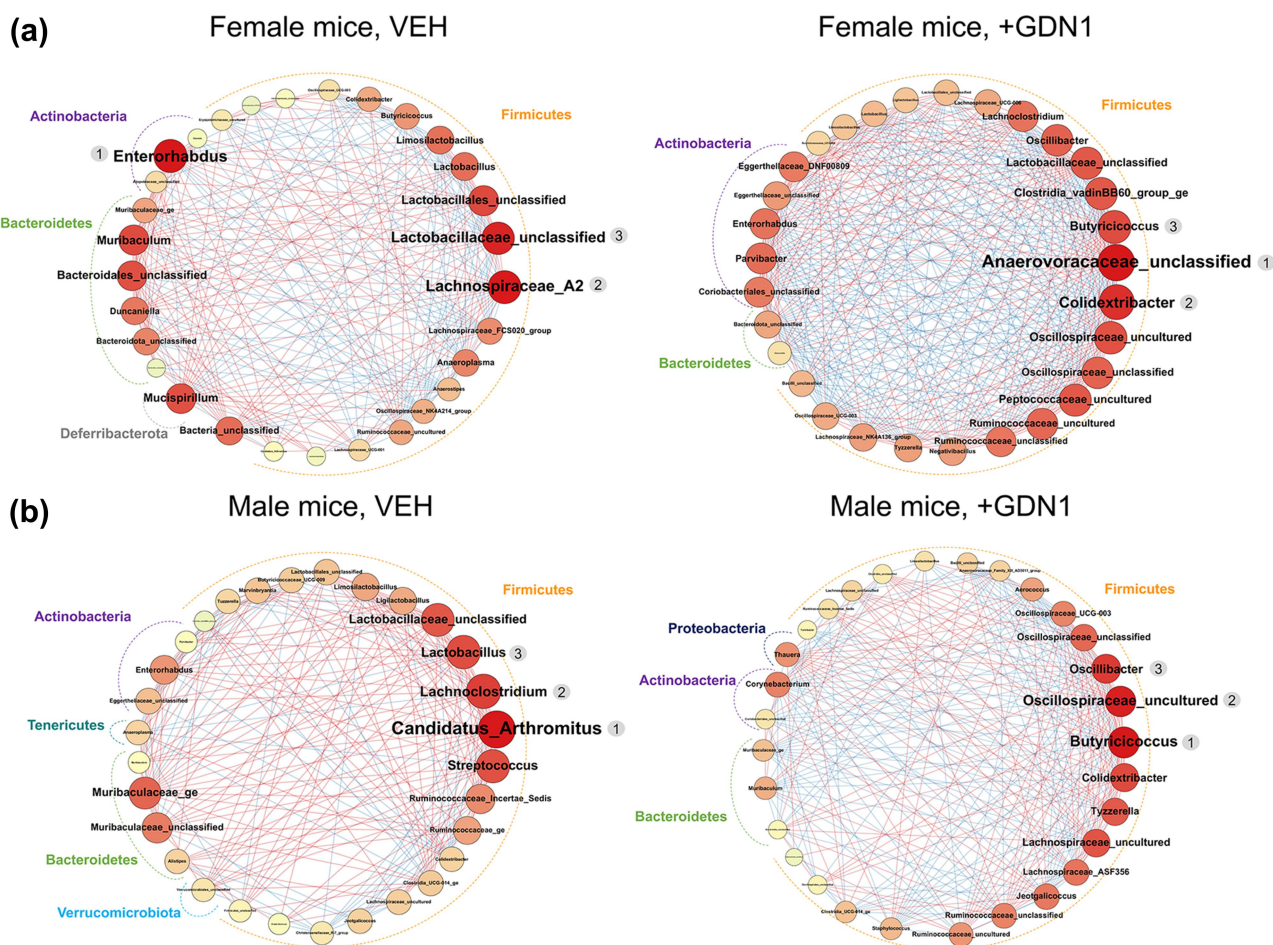


Figure 8. The microbial interaction networks identified in the female (A) and male (B) mice. potential microbial interactions were predicted using SparCC. nodes represent microbial genera, and only high-scoring eigenvector centrality nodes (top 30) are shown. eigenvector centrality is indicated by node size and color; a larger round node with a darker red hue corresponds to a higher value of eigenvector centrality. conversely, a smaller round node with a bright yellow hue corresponds to a lower value of eigenvector centrality. A node with the highest eigenvector centrality (rank 1, which is highly interacting with other nodes) may play a pivotal role in the network. A red edge depicts a positive interaction, whereas a blue edge depicts a negative interaction.

strain GDN1-administered male mice (Figure 8B; right panel), and this bacterial genus exhibited positive interactions (represented as red edges) with *Butyrificoccus* and 2 unclassified genera of Ruminococcaceae (Figures. 8B and S5).

Metabolite profile analysis of fecal extracts from the strain GDN1-administrated mice

To monitor the microbial activity of androgen catabolism in the mouse gut, fecal samples were extracted using ethyl acetate, and the androgenic metabolites were identified through UPLC – electrospray ionization (ESI)–HRMS (Figure 9). We employed extracted ion current (EIC) for m/z 305.21 (the most dominant ion peak of 2,3-SAOA) to detect 2,3-SAOA in the fecal extracts

of our male mice. In the fecal extract of the strain GDN1-administered male mice, we identified a compound with behaviors in UPLC (retention time = 7.1 min) and ESI – MS spectrum (quasimolecular adducts $[M + H]^+$ and $[M + Na]^+$ at m/z 323.22 and 345.20, respectively) matching with those of the authentic standard 2,3-SAOA (Figure 9A). By contrast, we did not detect any signals corresponding to 2,3-SAOA in the fecal extract of the vehicle-administered mice. Subsequently, we employed EIC for m/z 303.19 (the most dominant ion peak of 3,17-DHSA) to detect 3,17-DHSA in fecal extracts of our male mice. We detected this aerobic ring-cleaved metabolite in the fecal extract of the strain GDN1-administered male mice, with the UPLC – ESI–HRMS behaviors matching with those of the

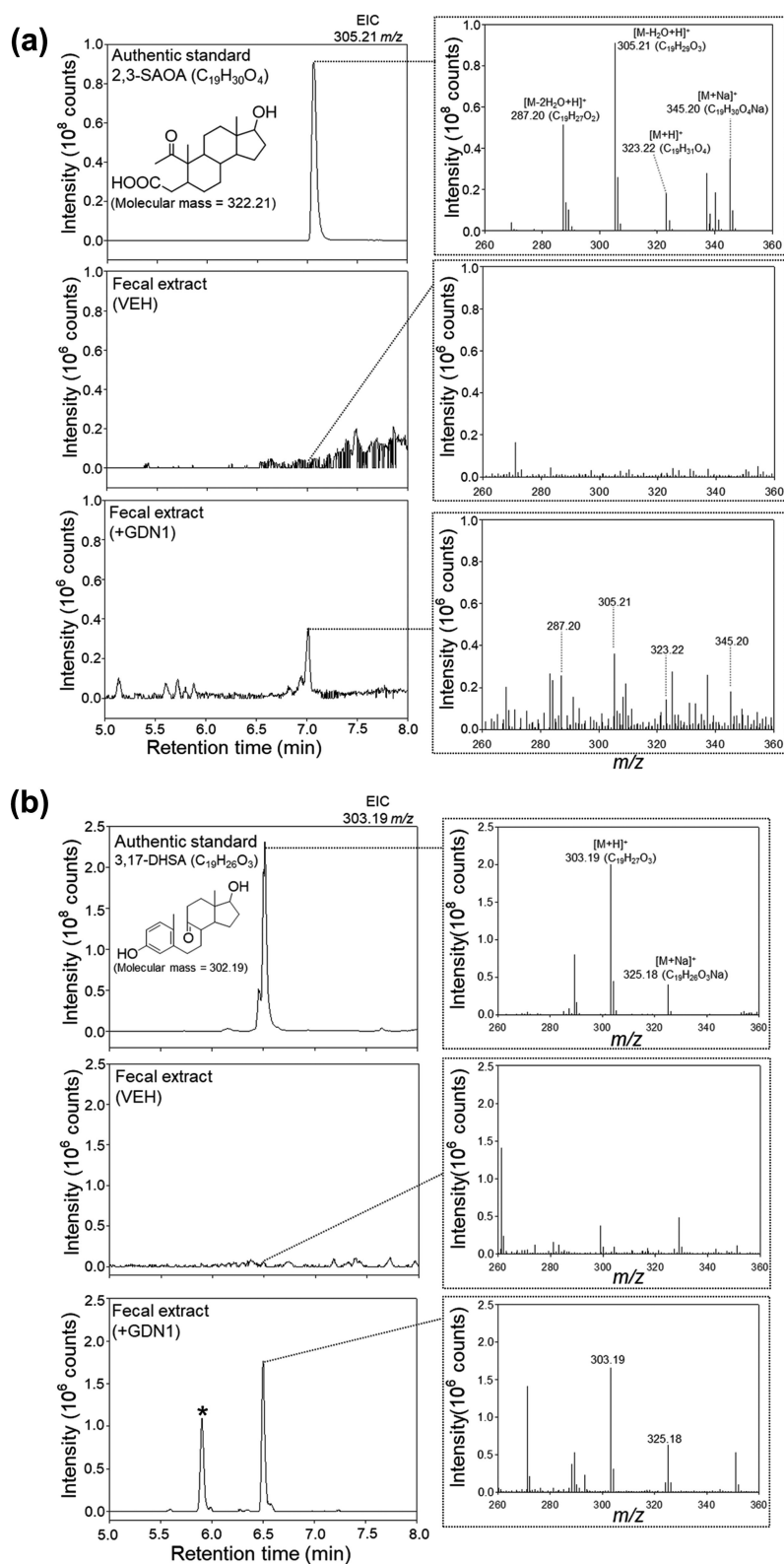


Figure 9. UPLC – ESI–HRMS detection of (A) 2,3-SAOA (anaerobic ring-cleaved metabolite) and (B) 3,17-DHSA (aerobic ring-cleaved metabolite) in the fecal extract of male mice administered with strain GDN1. Aforementioned ring-cleaved metabolites were not detected in the vehicle-administered mice. Fresh mouse feces were sampled 2 weeks after the first oral administration and was stored at -80°C before use. The fecal samples were extracted using ethyl acetate, and the androgen metabolites were analyzed through UPLC – ESI–HRMS. The predicted elemental composition of individual metabolite ions was calculated using MassLynx Mass Spectrometry Software (Waters); *unidentified metabolite.

authentic standard 3,17-DHSA (Figure 9B). The largest amount of 3,17-DHSA (980 ± 120 pg/g of feces) and 2,3-SAOA (70 ± 20 pg/g of feces) was determined in the mouse feces sampled after 2 weeks of the first oral administration. The metabolite profile analysis of the mouse fecal extracts thus suggests the production of both 3,17-DHSA and 2,3-SAOA (the aerobic and anaerobic ring-cleaved metabolites, respectively) in our male mice administered with strain GDN1.

Detection of inherent androgen catabolic gut microbes in the prostate cancer patients

Finally, we managed to investigate the prevalence of androgen catabolic gut microbes in male patients suffering from hyperandrogenism (Figure 10). Comparative genomic analysis of currently available bacterial genomes in the NCBI Genome database indicated that among the 26 *Thauera* genomes, only one strain (strain GDN1 in this study) contains both the anaerobic androgen catabolism genes *atcABC* and aerobic androgen catabolism genes *kshAB*, two strains (*T. butanivorans* strain NBRC 103,042 and *T. terpenica* strain 58Eu) harbor the *atcABC*, three strains exclusively harbor the *kshAB* (the gene synteny and the identity of their deduced amino acid sequences are shown in Figure 10A), while the remaining 20 (20/26; 77%) *Thauera* strains possess neither the *atcABC* nor *kshAB* (Fig. S7). Surprisingly, we could detect both the *atcABC* and *kshAB* genes in other denitrifying betaproteobacteria, including *Azoarcus* and *Aromatoleum* (Fig. S8). All three abovementioned genera belong to the bacterial order Rhodocyclales. This result thus suggests that *Thauera* is not the only gut microbe capable of androgen catabolism. The re-analysis of the gut microbiota from a previous study⁴³ indicates that the relative abundances of the genera *Aromatoleum* (0.0003%) and *Thauera* (0.0012%) in the prostate cancer patients ($n = 12$) are slightly higher than those (0.0002% and 0.0009%, respectively) of the healthy male ($n = 10$) in the same age range (62 ~ 77 years). However, the genus *Azoarcus* is hardly detected in the human gut. Similarly, at the bacterial order level, we observed a minor difference (statistically non-significant) in the Rhodocyclales abundance

between the prostate cancer patients (0.0015%) and healthy males (0.0012%).

Discussion

In this present study, we observed the occurrence of androgen catabolism in the animal gut. Our qPCR and PCR-based functional assay results suggested the presence of inherent *Thauera* spp. and *atcA*-like genes in the mouse gut. *Thauera* spp. are metabolically versatile and can grow with various hydrocarbons, including sugars, aromatics, and terpenoids, under aerobic, anaerobic, and fermentative conditions^{31,44,45}; these compounds are abundant in the gut of animals^{32–36}. However, the function of *Thauera* spp. in the animal gut remains unclear. Among the tested sex steroids, we found that strain GDN1 can only utilize androgens. The high substrate specificity of strain GDN1 thus excludes its potential adverse effects on estrogen and progesterone metabolism in the host. Strain GDN1 is efficient in catabolizing testosterone and ADD, but it is inefficient in catabolizing DHT. Both testosterone and ADD contain a double bond at C-4, while DHT contains a reduced A-ring structure. The oxidized A-ring (with double bonds at C-1 and/or C-4) is critical for many androgen catabolic enzymes such as *AtcABC*³⁰ and 3 β -hydroxysteroid dehydrogenase⁴⁶. The poor DHT utilization by strain GDN1 might be related to (i) strain GDN1 cannot efficiently import DHT into cells and/or (ii) androgen catabolic enzymes cannot efficiently degrade the DHT.

As abovementioned, *Thauera* species are metabolically versatile and their growth in the mouse gut does not necessarily depend on androgens. It is thus not a surprise that the expression of the strain GDN1 16S rRNA and *kshA* genes were respectively detected in the cecum and ileum. Likely, that the strain GDN1 does not use androgens as the sole carbon source in the cecum. The comparative transcriptomic analysis of strain GDN1 indicated that genes involved in the aerobic and anaerobic androgen catabolism are inducible and a major inducer includes testosterone. The *kshA* is critical for aerobic androgen catabolism; accordingly, its high expression was detected in the ileum where both oxygen and androgen (excreted from the bile) levels are relatively high in the ileum. Although

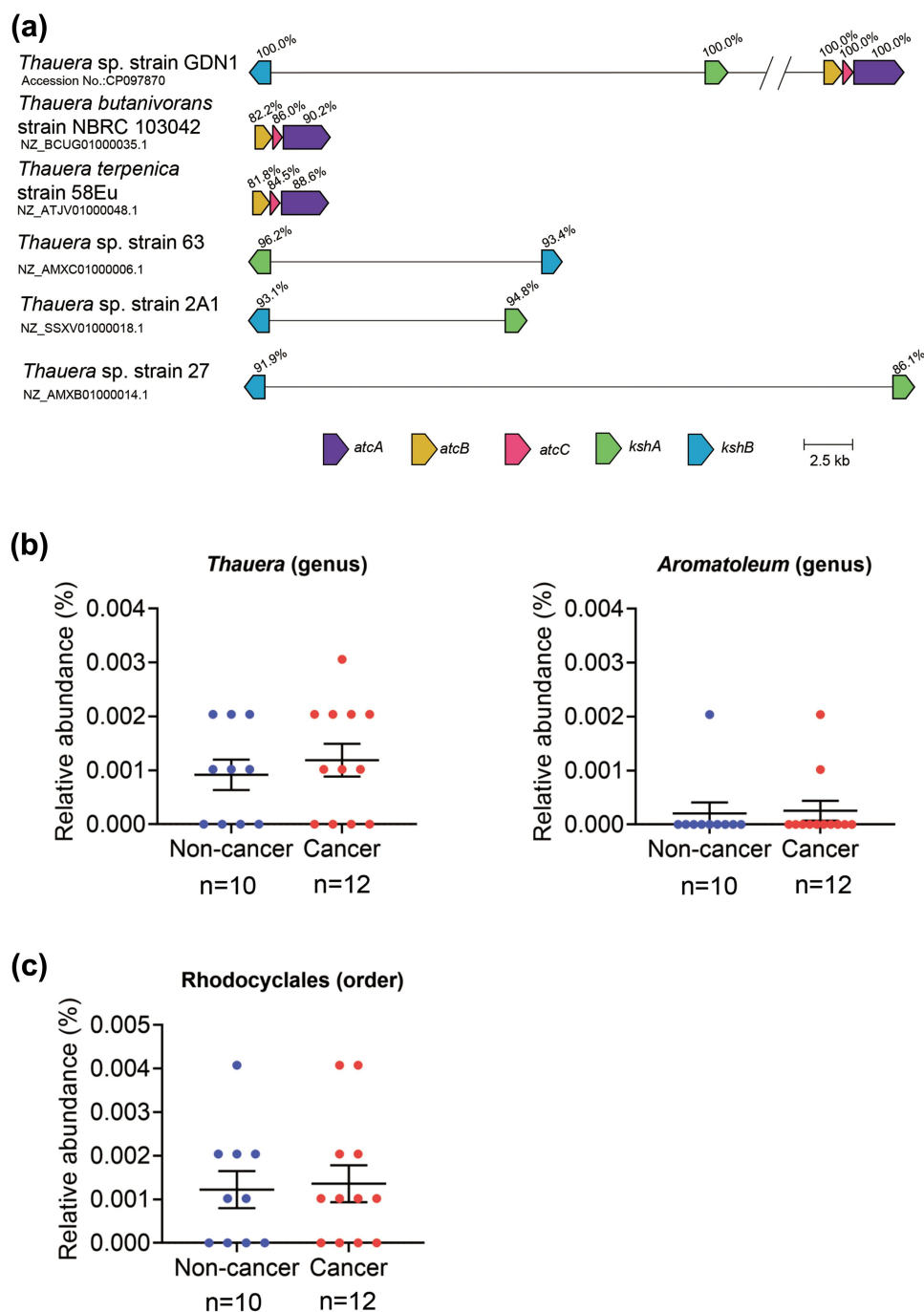


Figure 10. The prevalence of androgen catabolic bacteria in the human gut. (A) the distribution of the androgen catabolic genes *kshAB* and *atcABC* in the *Thauera* genomes. The cblaster software was used to search and visualize collocated protein-coding regions of androgen catabolic gene synteny in the *Thauera* RefSeq genomes. (B) the abundance of the genus *Thauera* and *Aromatoleum* (potential androgen degraders) in the prostatic cancer patients ($n = 12$) and healthy males ($n = 10$). (C) the abundance of the bacterial order Rhodocyclales (potential androgen degraders) in the prostatic cancer patients and healthy males. All data are shown as means \pm SEM. The significance was calculated using unpaired nonparametric t -test.

the expression of androgen catabolism genes of strain GDN1 is induced by testosterone, their expression was still observed in the acetate-grown cells at a basal level. Indeed, we detected the *atcA* expression at a low level in the mouse gut, mainly

in the cecum. The low *atcA* expression in the mouse gut was related to the extremely low testosterone content (<20 ng/g feces) in the lower GI tract⁴. The results of quantitative PCR-based functional assays thus suggest that androgen catabolism

by strain GDN1 mainly occurs in the ileum through the KshA-mediated catabolic pathway. Consistently, the metabolite profile analysis of the mouse feces also suggests 3,17-DHSA, the product of KshA, as the major androgenic metabolite.

The monitoring of microbial functional gene expression in the animal gut is challenging because of the highly dynamic gene expression of the gut microbiota⁴⁷. As an alternative approach, we applied UPLC – HRMS to detect *KshA* and *AtcA* products in the GI contents and feces of mice. However, the levels of androgen metabolites in the GI contents of our mice were too low to detect. Nonetheless, we detected the ring-cleaved metabolites 3,17-DHSA and 2,3-SAOA in the fecal extracts of the strain GDN1-administered mice, suggesting that both aerobic and anaerobic androgen catabolism occur in the mouse gut. Given that oxygenase-mediated steroid metabolism can proceed under microaerobic conditions⁴⁸, aerobic androgen catabolism might play a crucial role in gut androgen consumption, particularly in the ileum. Therefore, we believed that *kshA*-mediated aerobic androgen catabolism mainly occurs in the microaerobic ileum, and that *atcA*-mediated anaerobic androgen catabolism mainly occurs in the anaerobic cecum, where oxygen is often exhausted by gut microbes⁴⁹.

The highest copy number of the *Thauera* 16S rRNA was observed in the cecum of the strain GDN1-administered mice, indicating that strain GDN1 mainly inhabited the mouse cecum. Moreover, in the anaerobic (denitrifying) culture spiked with the mouse feces, we noted that strain GDN1 considerably consumed testosterone within 3 days, indicating the high survival rate of strain GDN1 in the mouse gut. Our qPCR and RT-qPCR results indicated that strain GDN1 mainly inhabited the mouse cecum, which has been considered the main location where steroids such as cholesterol and bile salts^{8–10} are reabsorbed through enterohepatic circulation. In animals, gut androgen content is typically quite low; to enable androgen catabolism, gut bacteria have to efficiently access, import, and accumulate this substrate from the environment. Steroid-catabolic bacteria often exhibit high cell surface hydrophobicity and high substrate uptake efficiency⁵⁰. Strain GDN1 may interrupt enterohepatic circulation through the adhesion, uptake, as well as aerobic and anaerobic

catabolism of gut androgens (mainly testosterone), leading to low androgen reabsorption into blood. Thus far, the information on the substrate uptake mechanisms and corresponding transporters of androgen-catabolic bacteria remains unclear.

The strain GDN1 administration caused a minor increase in the relative abundance of *Thauera* ($\leq 0.1\%$) in the gut microbiota. However, it profoundly affected the host physiology and gut bacterial community. For example, the strain GDN1 administration resulted in an increase in the number of negative interactions among gut microbial community, suggesting stronger competition between gut bacteria. Our data also indicate that strain GDN1-mediated changes in bacterial community structure are sex-dependent. In the strain GDN1-administered mice, the decreased abundance of Akkermansiaceae, Bifidobacteriaceae, and Enterobacteriaceae populations was observed. These gut bacteria have been reported to associate with circulating testosterone levels in mice and humans⁵¹. Moreover, members of Akkermansiaceae, Bifidobacteriaceae, and Enterobacteriaceae appear to play a role in prostate cancer progression^{52,53}. At the genus level, we identified *Thauera* (the only identified Proteobacteria member), *Butyrivibrio*, and unclassified genera of Ruminococcaceae as important microbes in the gut microbiota of strain GDN1-administered male mice, and *Thauera* exhibited positive interactions with these firmicutes. These firmicutes members often possess bacterial 20 β -hydroxysteroid dehydrogenase, which is involved in the microbial production of androgens through the steroid-17 α -desmolase pathway^{5,52}.

Our metagenomic re-analysis of the gut microbiota dataset from a previous study⁴³ indicates that *Thauera* inhabits the human gut in a low abundance. Moreover, we observed a slightly higher abundance (statistically non-significant) of *Thauera* in prostate cancer patients. However, this study sequenced the partial 16S rRNA gene (V1–V2 fragment; approximately 251 bp) of the gut microbiota on an Illumina platform; thus, the gut microbes could only be identified at genus or higher levels. Moreover, this study focused on 16S rRNA-based bacterial community structure analysis and functional genes from the gut microbiota were not available. Thus, there is no strong

evidence for the occurrence of *Thauera*-mediated androgen catabolism in the human gut. In addition to *Thauera*, androgen catabolism genes were identified in other denitrifying betaproteobacteria including *Azoarcus* and *Aromatoleum*. To monitor the androgen catabolic activity of human gut microbiota, the detection of both phylogenetic and functional genes is required. Microbial androgen catabolism in the human gut can be further supported through MS-based androgen metabolite profile analysis of human fecal samples.

Conclusions

The results of microbial community structure analysis suggest that androgen metabolism in mouse gut is achieved through synergistic microbial networks. In this study, we discovered the occurrence of androgen catabolism in the animal gut as well as the significant effect of this microbial activity on the regulation of host circulating androgens. Our biochemical and molecular data provided mechanistic insights into androgen-mediated gut microbe – host interactions along with the characteristic metabolites and functional genes for clinical diagnosis. This is important considering the future applications of androgen-catabolic bacteria as probiotics to reduce hyperandrogenism-associated host symptoms such as androgenetic alopecia, benign prostatic hypertrophy, and prostate cancer. Currently, androgen-deprivation therapy remains the mainstay of prostate cancer treatment. However, after an initial favorable response, patients often develop resistance to androgen-deprivation therapy, resulting in tumor progression, partially due to androgen production from steroidal precursors such as glucocorticoids and pregnenolone by some gut microbes^{5,52,53}. Therefore, new therapeutic strategies are urgently required. In addition, the redox reactions of androgens occurring in the animal gut may alter circulating testosterone levels and thus lead to adverse effects on host physiology¹⁴. In the animal gut, which has a highly reducing environment, testosterone is often reduced to DHT, the most potent natural androgen⁴. Therefore, gut microbes responsible for androgen reduction are often considered unfavorable species¹⁴. Our data indicate the

possible applicability of androgen-catabolic gut bacteria (e.g., strain GDN1) as potent probiotics in alternative therapy of hyperandrogenism.

Materials and methods

Chemicals

The [2,3,4C-¹³C]testosterone was purchased from Isosciences. Commercially available steroid standards [androstadienedione (ADD), androstenedione (AD), cholesterol, dihydrotestosterone (DHT), estradiol, 17 α -ethinylestradiol, progesterone, and testosterone] were purchased from Sigma-Aldrich (St. Louis, MO, USA). The androgenic ring-cleaved metabolites 3,17-DHSA and 2,3-SAOA were produced as described elsewhere²⁹. Other chemicals used were of analytical grade and were purchased from Mallinckrodt Baker (Phillipsburg, USA), Merck Millipore (Burlington, USA), and Sigma-Aldrich unless specified otherwise.

Detection of androgen metabolites and determination of androgenic activity in the denitrifying strain GDN1 culture

Denitrifying strain GDN1 (500 mL, initial OD_{600 nm} = 0.2) was incubated at 37°C and pH 6.0 with testosterone (1 mM) and nitrate (10 mM) in a chemically defined medium as described elsewhere³¹. 17 α -Ethinylestradiol (final concentration = 50 μ M), which cannot be utilized by strain GDN1, was added to the bacterial culture to serve as an internal control. Cultural samples (5 mL each) were withdrawn every 8 h (0 ~ 48 h). The pH of the cultural samples (1 mL) was adjusted to pH < 2 using 5 M HCl. The acid-treated cultures were extracted three times with the same volume of ethyl acetate to recover the residual testosterone and its derivatives from the aqueous phase. The testosterone-derived intermediates extracted from the cultural samples were identified and quantified using UPLC – HRMS. The protein and nitrate contents of strain GDN1 cultures were determined as described below. The remaining cultural samples (1 mL) were extracted with ethyl acetate three times. After the solvent was completely evaporated, the residue was re-dissolved in 10 μ L of dimethyl

sulfoxide (DMSO) to determine its androgenic activity (see below).

Aerobic growth of strain GDN1 on testosterone

Strain GDN1 was aerobically grown in a phosphate-buffered shake-flask (300 ml in 1 L-Erlenmeyer flask) containing 1 mM testosterone. 17α -Ethinylestradiol (50 μ M; indigestible by strain GDN1) was added as an internal control. Nitrate was omitted from the medium. In 1 L of distilled water, the medium contained the following: 0.29 g testosterone, 2.0 g NH_4Cl , 0.5 g $\text{MgSO}_4 \cdot 7 \text{H}_2\text{O}$, and 0.1 g $\text{CaCl}_2 \cdot 2 \text{H}_2\text{O}$. After autoclaving, sterile 50 ml KH_2PO_4 - K_2HPO_4 buffer solution (1 M, pH 6.0), vitamins (1 mL/L)⁵⁴, EDTA-chelated mixture of trace elements (1 mL/L)⁵⁵, and selenite and tungstate solution (1 mL/L)⁵⁶ were added. The aerobic culture was incubated at 37°C in an orbital shaker (180 rpm). The cultural samples (5 mL) were withdrawn every 6 h (0 ~ 30 h). The testosterone-derived intermediates extracted from the cultural samples were identified and quantified using UPLC – HRMS. The androgenic activity of the cultural samples was determined as described later.

Measurement of protein content and nitrate concentration

Strain GDN1 cultural samples or cell suspension (0.2 mL) were centrifuged at $10,000 \times g$ for 10 min. After centrifugation, the cell pellet was resuspended in 1 mL of reaction reagent (Pierce BCA protein assay kit; Thermo Scientific). The protein content was determined using a BCA protein assay according to manufacturer's instructions with bovine serum albumin as the standard. The supernatant (0.1 mL) was diluted with 0.9 mL of double-distilled water, and the nitrate was determined using the cadmium reduction method according to manufacturer's instructions (Nitrate Reagent Kit HI93728–01, Hanna Instruments).

lacZ-based yeast androgen bioassay

The yeast androgen bioassay was conducted as described elsewhere³⁹. Briefly, the individual androgen standards or cell extracts were dissolved in DMSO, and the final concentration of DMSO in

the assays (200 μ L) was 1% (v/v). The resulting DMSO solutions (2 μ L) were added to yeast cultures (198 μ L, initial $\text{OD}_{600 \text{ nm}} = 0.5$) in a 96-well microtiter plate. The β -galactosidase activity was determined after 18 h incubation at 30 °C. The yeast suspension (25 μ L) was added to a Z buffer (225 μ L) containing *o*-nitrophenol- β -D-galactopyranoside (ONPG, 2 mM), and the reaction mixtures were incubated at 37 °C for 30 min. After the reactions were stopped by adding 100 μ L of 1 M sodium carbonate, the amount of yellow-colored nitrophenol product was measured at 420 nm on a microplate spectrophotometer.

Analytical chemical methods

(a)Thin-layer Chromatography (TLC)

The steroid standards and products were separated on a silica gel-coated aluminum TLC plate (Silica gel 60 F₂₅₄; thickness, 0.2 mm; 20 × 20 cm; Merck) using dichloromethane:ethyl acetate:ethanol (14:4:0.05, v/v/v) as the developing phase. The steroids were visualized under UV light at 254 nm or by spraying the TLC plates with 30% (v/v) H_2SO_4 , followed by an incubation for 1 min at 100°C (in an oven).

(b)High-Performance Liquid Chromatography (HPLC)

A reversed-phase Hitachi HPLC system equipped with an analytical RP-C₁₈ column [Luna 18(2), 5 μ m, 150 × 4.6 mm; Phenomenex] was used for separating steroid metabolites in this study. The separation was achieved isocratically using a mobile phase of 45% methanol (v/v) at 35°C at a flow rate of 0.5 mL/min. The steroid metabolites were detected using a photodiode array detector (200–450 nm). In some studies, HPLC was also used for quantifying steroids extracted from the strain GDN1 cultures. The quantity of major androgens (AD, ADD, DHT, and testosterone) was determined using a standard curve generated from individual steroid standards. The R^2 values for the standard curves were >0.98. The presented data are the average values of three experimental measurements.

(c)Ultra-Performance Liquid Chromatography – High-Resolution Mass Spectrometry (UPLC – HRMS)

The androgen metabolites in mouse fecal (0.1 g) or serum (0.2 mL) samples were extracted using ethyl

acetate for three times. Before the extraction, 0.1 ng of [2,3,4C-¹³C]testosterone (internal standard) was added to the samples. After the solvent was evaporated, the residue was re-dissolved in 10 µL of methanol. The androgen metabolites were identified by comparing their corresponding retention time and *m/z* values to the authentic standards. The androgen metabolites were quantified using the standard curves established using the authentic standards (linear range: 0.05–20 ng/mL; 2-fold serial dilution).

Androgen metabolites were analyzed using UPLC – HRMS on a UPLC system coupled to either an Electric Spray Ionization – Mass Spectrometry (ESI – MS) system or an Atmosphere Pressure Chemical Ionization – Mass Spectrometry (APCI – MS) system. Androgen metabolites were firstly separated using a reversed-phase C₁₈ column (Acquity UPLC® BEH C18; 1.7 µm; 100 × 2.1 mm; Waters) at a flow rate of 0.4 mL/min at 35°C (oven temperature). The mobile phase comprised a mixture of two solutions: solution A [0.1% formic acid (v/v) in 2% acetonitrile (v/v)] and solution B [0.1% formic acid (v/v) in methanol]. Separation was achieved using a gradient of solvent B from 10% to 99% in 8 min. ESI – HRMS analysis was performed using a Thermo Fisher Scientific™ Orbitrap Elite™ Hybrid Ion Trap-Orbitrap Mass Spectrometer (Waltham, MA, USA). Mass spectrometric data in positive ionization mode were collected. The source voltage was set at 3.2 kV; the capillary and source heater temperatures were 360°C and 350°C, respectively; the sheath, auxiliary, and sweep gas flow rates were 30, 15 and 2 arb units, respectively. APCI – HRMS analysis was performed using a Thermo Fisher Scientific™ Orbitrap Elite™ Hybrid Ion Trap-Orbitrap Mass Spectrometer (Waltham, MA, USA) equipped with a standard APCI source. Mass spectrometric data in positive ionization mode (parent scan range: 50–600 *m/z*) were collected. The capillary and APCI vaporizer temperatures were 120°C and 400°C, respectively; the sheath, auxiliary, and sweep gas flow rates were 40, 5 and 2 arbitrary units, respectively. The source voltage was 6 kV and the current was 15 µA. The elemental composition of individual adduct ions

was predicted using Xcalibur™ Software (Thermo Fisher Scientific).

General molecular biological methods

The strain GDN1 genomic DNA was extracted using the Presto™ Mini gDNA Bacteria Kit (Geneaid, New Taipei City, Taiwan). PCR mixtures (50 µL) contained nuclease-free H₂O, 2 × PCR master mix (Invitrogen™ Platinum™ Hot Start PCR 2× Master Mix, Thermo Fisher Scientific, Waltham, MA, USA), forward and reverse primers (200 nM each), and template DNA (10–30 ng). The PCR products were verified using standard TAE-agarose gel (1.5%) electrophoresis with the SYBR® Green I nucleic acid gel stain (Invitrogen Thermo Fisher Scientific, Waltham, MA, USA), and the PCR products were purified using the GenepHlow Gel/PCR Kit (Geneaid, New Taipei City, Taiwan). The TA cloning was performed with T&A™ Cloning Vector Kit (YEASTERN BIOTECH, New Taipei City, Taiwan).

PacBio sequencing of the strain GDN1 genome

For library preparation and PacBio sequencing, approximately 1 µg of strain GDN1 genomic DNA was sheared by Covaris g-TUBE (Covaris, Woburn, MA, USA) and purified via AMPure PB beads (PacBio, Menlo Park, CA, USA). The sheared and purified DNA fragments were used as templates to prepare the SMRTbell library through SMRTbell template prep kit 1.0 (PacBio, Menlo Park, CA, USA), according to the manufacturer's instructions. After adaptor-ligation to the inserts, the inserts with suitable size for sequencing were selected with the BluePippin system. The SMRT sequencing was performed on SMRT 1 M Cell v3 (PacBio, Menlo Park, CA, USA) with chemistry version 3.0 on PacBio Sequel sequencer (Genomics BioSci & Tech Co). A primary filtering analysis was achieved on the Sequel System, and the secondary analysis was completed using the SMRT analysis pipeline version 8.0. For the genome assembly, the filtered subreads after SMRT Link v8.0 were assembled by a long-read assembly algorithm Flye v2.7⁵⁷. The SSPACE-LongRead

v1.1⁵⁸ was applied for draft genome scaffolding and PBjelly v15.8.24 was used for gap closure^{58,59}. Subsequently, genome polishing was conducted with Arrow v2.3.3 software (PacBio, Menlo Park, CA, USA). A further assembly of the circularizing genome was conducted using Circlator v1.5.5⁶⁰. Finally, the quality of the assembled genome was evaluated by QUAST v4.5⁶¹. After the *de novo* genome assembly, the annotations of genomic bacterial features were achieved with Prokka v1.13⁶².

RNA extraction and comparative transcriptomic analysis

The transcriptomes were extracted from the strain GDN1 cells grown aerobically or anaerobically with acetate (10 mM) or testosterone (2 mM) as the sole carbon source. The transcriptomes were extracted using the Direct-zol RNA MiniPrep Kit (Zymo Research, Irvine, CA, USA), and were further purified using Turbo DNA-free Kit (Thermo Fisher Scientific, Waltham, MA, USA) to eliminate DNA. rRNA was removed from the transcriptome samples using the Ribo-Zero rRNA Removal Kit (Epicenter Biotechnologies; Madison, WI, USA). The quality of the resulting RNA library was assessed on a Bioanalyzer 2100 system (Agilent Technologies, CA, USA) by using the RNA Nano 6000 Assay Kit. Only the samples with an integrity value in the range between 8 to 10 were selected for further transcriptomic analysis. First-strand cDNA was synthesized using the purified transcriptomes as the templates. Second-strand cDNA was synthesized in a reaction mixture containing Second-Strand Synthesis Kit (New England Biolabs; Ipswich, MA, USA). cDNA was purified using the Qiagen purification kit, followed by end repair using NEBNext® End Repair Module (New England Biolabs). Antisense strand DNA was digested in the samples using the Uracil-Specific Excision Reagent Enzyme Kit (New England Biolabs), followed by a PCR to amplify the cDNA. The constructed sequencing libraries were sequenced as paired-end reads (with 150–200 bp read length) on the Illumina NovaSeq 6000 system (Illumina; San Diego, CA). Raw reads were first processed through in-house scripts (Novogen, Singapore), and the adapters were removed. In addition, reads with uncertain

nucleotides (N) more than 10% or reads with low-quality nucleotides (base quality<5; constituting>50% of the reads) were discarded. More than 98.2% of qualified read pairs were kept for mapping against strain GDN1 genome using Bowtie2 (version 2.2.3). The mismatch parameter is set to two, and other parameters are set to default. Finally, more than 96% of the total reads were aligned to the strain GDN1 genome (Table S1). The mapping results were quantified using the python script *htseq-count* (<https://htseq.readthedocs.io/en/master/>) and gene expression levels were estimated using fragments per kilobase of transcript per million mapped reads (FPKM).

Preparation of strain GDN1 cell suspension for mice administration

Strain GDN1 was aerobically grown in tryptone soy broth (700 mL), and the bacterial cultures were incubated at 37°C in an orbital shaker (180 rpm). The bacterial cells were harvested at log phase ($OD_{600\text{ nm}} = 0.5 \sim 0.7$) through centrifugation, and the cell pellet was washed and resuspended in a denitrifying mineral medium (500 mL) containing 0.2 mM testosterone (the inducer of androgen catabolic genes). The denitrifying strain GDN1 cultures were incubated at 37°C with shaking. The strain GDN1 cultures were sampled (1 mL each) twice per day, and the residual testosterone was determined using HPLC. When testosterone was exhausted (approximately 3 days), the strain GDN1 cells were washed twice using basal mineral medium (composed of 4.0 g NH_4Cl , 4 g $\text{MgSO}_4 \cdot 7\text{H}_2\text{O}$, 0.8 g $\text{CaCl}_2 \cdot 2\text{H}_2\text{O}$, 4.2 g NaHCO_3 and 1.7 g KH_2PO_4 per liter of distilled water), and then resuspended in the same mineral medium (adjusted to $OD_{600\text{ nm}} = 2$). The colony-formation-units (CFUs) of the resulting cell suspension were determined by counting the numbers of strain GDN1 colonies grown on tryptone soy agar. This cell suspensions of strain GDN1 were stored at 4°C (within 5 days) before use.

GDN1 administration through oral gavage

C57BL/6J mice (aged 7-week-old) were obtained from the Animal Center of the Medical College (National Taiwan University, Taipei, Taiwan) and

were kept in standard animal housing conditions with the health guidelines for the care and use of experimental animals. The experiments were approved by the local ethics committee (IACUC No. 20210326). After acclimatization for one week, female and male mice with similar body weight (16–18 g) were randomly assigned into two treatment groups [vehicle-administered mice (VEH) or strain GDN1-administered mice (+GDN1)]. For administration of strain GDN1, approximately 5×10^8 CFUs (suspended in 200 μ L of basal mineral medium) were fed into each mouse through oral gavage twice per week (Figure 4A). The same volume of sterilized basal mineral medium was administered to the vehicle mice. During the period of continuous administration, the drinking water for mice was supplemented with sodium nitrate (2 mM). Fresh mouse feces were collected daily, and the body weight was measured once per week. Mice were sacrificed on day 25 (anesthetized with 3% isoflurane) and the mouse blood was collected through cardiac puncture. The mouse gastrointestinal (GI) tracts, including the ileum, cecum, and colon, were dissected to obtain the GI contents (for bacterial DNA and RNA extraction). All the mouse samples, including serum, feces, and GI contents, were stored at -80°C before use.

Determination of serum testosterone and estradiol levels using ELISA

The serum testosterone level of mice was determined using a competitive binding Testosterone Parameter Assay Kit (R&D Systems, Minneapolis, MN) according to the manufacturer's instructions with testosterone as the standard. The minimum detectable dose of testosterone for the ELISA kit was approximately 0.03 ng/mL. The following compounds were tested for their cross-reactivity (testosterone cross-reactivity was set as 100%): DHT (2.6%), AD (<0.1%), 17β -estradiol (<0.1%), and progesterone (<0.1%). On the other hand, the serum estradiol level of mice was determined using a competitive binding Estradiol Parameter Assay Kit (R&D Systems, Minneapolis, MN) according to the manufacturer's instructions with 17β -estradiol as the standard. The minimum detectable dose of estradiol was approximately 5 pg/mL. The following compounds were tested for cross-reactivity (17β -

estradiol cross-reactivity was set as 100%): estrone (0.26%), estriol (0.86%), 17α -ethinylestradiol (<0.1%), and progesterone (<0.1%).

Extraction of bacterial DNA from mouse fecal samples and GI content

Bacterial DNA in the mouse fecal samples and GI content (200 mg) was extracted using QIAamp® PowerFecal® Pro DNA kit (Qiagen, Hilden, Germany) according to the manufacturer's instructions. The DNA concentration was determined using NanoDrop Spectrophotometer ND-1000 or Qubit™ dsDNA Assay kit (Invitrogen Thermo Fisher Scientific, Waltham, MA, USA).

Extraction of bacterial RNA from mouse GI content and reverse transcription of the RNA

Bacterial RNA from mouse GI contents (approximately 250 mg) was extracted using RNeasy® PowerMicrobiome® kit (Qiagen, Hilden, Germany) according to the manufacturer's instructions. To confirm the complete DNA elimination, the resulting RNA samples were amplified using bacterial universal 16S rRNA primers 27F and 1492 R as described elsewhere³¹. The RNA concentration was determined using NanoDrop Spectrophotometer ND-1000 or Qubit™ HS RNA Assay kit (Invitrogen Thermo Fisher Scientific, Waltham, MA, USA). The quality of the bacterial RNA samples was examined based on the ratio of 23S/16S rRNA separated through agarose-electrophoresis⁶³. Bacterial RNA (1 μ g) was reverse-transcribed using SuperScript™ IV kit (Invitrogen Thermo Fisher Scientific, Waltham, MA, USA) according to the manufacturer's instructions. The resulting cDNA was used for the quantitative PCR (qPCR).

Real-time qPCR

The bacterial DNA or cDNA was quantified through qPCR by using the Power® SYBR Green PCR Master Mix (Applied Biosystem, Thermo Fisher Scientific, Waltham, MA, USA) on the QuantStudio 5 platform (Applied Biosystem, Thermo Fisher Scientific, Waltham, MA, USA)

according to the manufacturer's instructions. Primers used for the qPCR are shown in Table S2. To determine the abundance of *Thauera* species in the mouse feces and GI contents, a real-time qPCR-based assay⁶⁴ was performed; a calibration curve was obtained by using 10-fold serial dilution of plasmid DNA carrying a cloned strain GDN1 16S rRNA gene. To quantify the expression of androgen catabolic genes *atcA* and *kshA* in the mouse GI tract (ileum, cecum, and colon), the relative change of gene expression was calculated using the $2^{-\Delta\Delta C_t}$ method⁴² with the Ct value of bacterial universal 16S rRNA (see Table S2 for nucleotide sequences) as the internal control. The expression of individual androgen catabolic genes in the VEH ileum was set as 1.

Bacterial 16S rRNA sequencing and data processing

For bacterial 16S rRNA sequencing, the hypervariable (V3-V4) region was amplified using the primer set (16S-341F/805 R, see Table S2 for nucleotide sequences) according to the 16S Metagenomic Sequencing Library Preparation procedure (Illumina; San Diego, CA). The success of PCR amplification was confirmed using agarose electrophoresis (1.5%), and the PCR products with a size of approximately 500-bp were selected and purified using the AMPure XP beads. The resulting PCR products were ligated to the dual indices and Illumina sequencing adapters with Nextera XT Index Kit. The quality of indexed PCR products was examined on the Qubit 4.0 Fluorometer (Invitrogen Thermo Fisher Scientific, Waltham, MA, USA) and Qsep100TM Capillary electrophoresis system (Bioptic Inc. New Taipei City, Taiwan). The purified indexed PCR products were further processed according to the Illumina standard protocol, and sequenced on an Illumina MiSeq platform (paired-end 2×300 bp) at the BIOTOOLS Co., Ltd (New Taipei City, Taiwan).

The raw Illumina amplicon reads were quality-filtered and analyzed using mothur v1.46.1 according to mothur MiSeq standard operating procedure⁶⁵. In brief, the forward and reverse Fastq files were merged; the resulting sequences with low quality (quality score < 30), merged sequences with a length < 400 bp or > 600 bp, sequences containing nucleotide repeats (> 8), and

primer sequences were all removed from the dataset. The sequences were further denoised using *pre.cluster* command and amplicon sequence variants (ASVs) were generated with two base-pair differences. Chimeric sequences were removed using VSEARCH algorithm (*chimera.vsearch*) within mothur. The ASVs were assigned into a taxonomic hierarchy based on the reference sequences from the SILVA database (version 138_1) using mothur (*classify.seqs*). Sequences classified as chloroplast, eukaryote, mitochondria, or unknown were removed from the dataset (*remove.lineage*). To normalize the dataset, each sample was rarefied to the minimum of 48,558 for downstream analysis (*sub.sample*).

Gut bacterial community structure analysis and the construction of microbial interaction networks

To evaluate beta-diversity, we used non-metric multidimensional scaling (NMDS) ordination approach based on Bray-Curtis dissimilarities to assess the composition of bacterial communities between the vehicle and strain GDN1 treatments. The NMDS was calculated using the *vegan* package in R studio⁶⁶. The significant changes in bacterial community structure were assessed using permutational analysis of variance (PERMANOVA) in R studio using the package *vegan*. DESeq2 was used to analyze the differential abundance of bacterial taxa (i.e., Phylum and Family levels) between the vehicle and strain GDN1 treatments based on Benjamini-Hochberg adjusted p-value to reduce false discovery rate (FDR)⁶⁷. The top 5 highly abundant bacterial phyla were visualized as histograms, whereas the bacterial families that were significantly different between groups were visualized as heatmaps using ClustVis⁶⁸. To simulate potential interactions between different bacterial genera, we generated SparCC networks with 1000 permutations based on centered log-ratio transform data and spearman correlations⁶⁹ in R studio using the package *SpiecEasi*⁷⁰. SparCC values with p-value less than 0.05 were considered significant, and were selected to generate bacterial interaction networks in Gephi⁷¹. Node centralities such as degree, closeness, betweenness, and eigenvector were calculated in Gephi⁷¹. The bacterial genera with potential important roles in a network were

selected based on their eigenvector centrality values.⁷² A high eigenvector centrality value indicates relatively high degree, closeness, and betweenness centrality values. The top 30 bacterial genera with the highest eigenvector centrality value were selected to visualize the network. Eigenvector centrality is indicated by node size and color: a larger round node with a darker red hue corresponds to a higher value of eigenvector centrality. Conversely, a smaller round node with a bright yellow hue corresponds to a lower value of eigenvector centrality. A red edge depicts a positive interaction, while a blue edge depicts a negative interaction.

Comparative genomic analysis of the androgen catabolic bacteria

The deduced amino acid sequences of the androgen catabolism genes *atcABC* and *kshAB* from strain GDN1 were used as queries to search against a local sequence database. This database was downloaded and constructed from 25 NCBI available *Thauera* RefSeq genomes. All the processes mentioned above were executed by the cblaster software⁷³. The homologous hit was set to 1, and sequence identity was larger than 60%. In addition, the gap of any two hits in a gene synteny was set to 10⁷⁴ Mb to cover all potential candidates. The cblaster was also applied to search other genomes with the same criteria but fully remote searches against public NCBI RefSeq genomes⁷⁵.

Re-analysis of gut microbiota in prostate cancer patients

The FASTQ files in the BioProject PRJDB10718⁴³ were downloaded and analyzed using mothur. The FASTQ files were quality filtered using the “screen.seqs” command to remove sequences with ambiguous bases and those with repeated nucleotides (<8). Quality-filtered sequences were dereplicated using the “unique.seq” command and the sequences were aligned with a custom-made reference database (i.e., Silva reference database release 138.1 with 5 additional 16S rRNA sequences: *Thauera* sp. strain GDN1, *Azoarcus* sp. strain Aa7, *Azoarcus* sp. strain DN11, *Azoarcus* sp. strain

CIB, and *Aromatoleum anaerobium* LuFRes1. Subsequently, the aligned sequences were pre-clustered using the “pre.cluster” command to generate ASVs with 2 base-pair differences between sequences. The ASVs were classified using the custom-made reference database. Sequences classified as chloroplast, mitochondria, unknown, archaea, or eukaryota were removed from the dataset. The number of sequences from each sample was rarefied to an equal sequencing depth (98144 reads). Finally, the relative abundance of individual bacterial taxa (e.g., *Thauera*, *Aromatoleum*, *Azoarcus*, or Rhodocyclales) was calculated; namely, the number of each taxon was divided by the total sequence number (i.e., 98144).

Statistical analyses

All the biological experiments were repeated in at least triplicate. The probability value (*p* value) was examined by Welch’s *t* test or nonparametric Mann-Whitney U test using GraphPad Prism 8.

Acknowledgments

We thank the Small Molecule Metabolomics core facility sponsored by the Institute of Plant and Microbial Biology (IPMB), Academia Sinica for UPLC–HRMS analysis.

Authors’ contributions

T.-H.H., C.-H.C., M.-J.C., and Y.-R.C. designed research; T.-H.H., C.-H.C., Y.-L.C., G.-J.B.-M., T.-Y.W., P.-T.L., C.-W.L., Y.-L.L., P.-H.C., and Y.-L.T. performed research; P.-H.W., T.-H.L., and C.-J.S. contributed new reagents/analytic tools; C.-H.C., Y.-L.C., M.-J.C. and Y.-R.C. analyzed data; and T.-H.H., P.-H.W. and Y.-R.C. wrote the paper.

Disclosure statement








No potential conflict of interest was reported by the authors.

Funding

This study was supported by the Ministry of Science and Technology of Taiwan (MOST 110-2311-B-001-033-MY3, 109-2314-B-002-125-MY3, 110-2811-B-002-562, and 110-2222-E-008-002) and Academia Sinica Career Development Award (AS-CDA-110-L13). We thank the Small Molecule

Metabolomics core facility sponsored by the Institute of Plant and Microbial Biology (IPMB), Academia Sinica for UPLC–HRMS analysis.

ORCID

Tsun-Hsien Hsiao  <http://orcid.org/0000-0003-2002-2760>
 Yi-Lung Chen  <http://orcid.org/0000-0001-7840-7423>
 Po-Hsiang Wang  <http://orcid.org/0000-0001-9900-0972>
 Guo-Jie Brandon-Mong  <http://orcid.org/0000-0002-1673-8021>
 Chao-Jen Shih  <http://orcid.org/0000-0001-7791-8264>
 Mei-Jou Chen  <http://orcid.org/0000-0002-2305-1105>
 Yin-Ru Chiang  <http://orcid.org/0000-0001-6899-3166>

Data availability statement

Oligonucleotide primers used in this study are listed in Table S2. Nucleotide sequences of the 16S rRNA and androgen catabolism genes of strain GDN1 are shown in Appendices S1–S3. Transcriptomic data of the strain GDN1 are available in Dataset S1. Genome sequence of the strain GDN1 (accession no. CP097870) has been deposited in the National Center for Biotechnology Information (NCBI) Genome database. The transcriptomes of the strain GDN1 have been deposited in the NCBI SRA database under BioProject ID PRJNA838737 [accession numbers: SRR19418054~SRR19418057]. The fecal bacterial 16S rRNA sequencing datasets have been deposited in the NCBI SRA database under BioProject ID PRJNA838737 [accession numbers: SRR19913488~SRR19913535].

References

- Doyle WI, Meeks JP. Excreted steroids in vertebrate social communication. *J Neurosci.* 2018;38(14):3377–3387. doi:10.1523/JNEUROSCI.2488-17.2018.
- Trüeb RM. Molecular mechanisms of androgenetic alopecia. *Exp Gerontol.* 2002;37(8–9):981–990. doi:10.1016/S0531-5565(02)00093-1.
- Russell DW, Wilson JD. STEROID 5 α -REDUCTASE: TWO GENES/TWO ENZYMES. *Annu Rev Biochem.* 1994;63(1):25–61. doi:10.1146/annurev.bi.63.070194.000325.
- Collidén H, Landin A, Wallenius V, Elebring E, Fändriks L, Nilsson ME, Ryberg H, Poutanen M, Sjögren K, Vandenput L, et al. The gut microbiota is a major regulator of androgen metabolism in intestinal contents. *American Journal of Physiology-Endocrinology and Metabolism.* 2019;317(6):E1182–92. doi:10.1152/ajpendo.00338.2019.
- Pernigoni N, Zagato E, Calcinotto A, Troiani M, Mestre RP, Cali B, Attanasio G, Troisi J, Minini M, Mosole S, et al. Commensal bacteria promote endocrine resistance in prostate cancer through androgen biosynthesis. *Science.* 2021;374(6564):216–224. doi:10.1126/science.abf8403.
- Wu C, Wei K, Jiang Z. 5 α -reductase activity in women with polycystic ovary syndrome: a systematic review and meta-analysis. *Reprod Biol Endocrinol.* 2017;15(1):21. doi:10.1186/s12958-017-0242-9.
- Auer KE, Kußmaul M, Möstl E, Hohlbaum K, Rüllicke T, Palme R. Measurement of fecal testosterone metabolites in mice: replacement of invasive techniques. *Animals (Basel).* 2020;10(1):165. doi:10.3390/ani10010165.
- Adlercreutz H, Martin F, Järvenpää P, Fotsis T. Steroid absorption and enterohepatic recycling. *Contraception.* 1979;20(3):201–223. doi:10.1016/0010-7824(79)90094-5.
- Cai J-S, Chen J-H. The mechanism of enterohepatic circulation in the formation of gallstone disease. *J Membr Biol.* 2014;247(11):1067–1082. doi:10.1007/s00232-014-9715-3.
- Lu K, Lee MH, Patel SB. Dietary cholesterol absorption; more than just bile. *Trends Endocrinol Metab.* 2001;12(7):314–320. doi:10.1016/S1043-2760(01)00433-7.
- Hugenholtz F, de Vos WM. Mouse models for human intestinal microbiota research: a critical evaluation. *Cell Mol Life Sci.* 2018;75(1):149–160. doi:10.1007/s00018-017-2693-8.
- Nakayama A, Eguchi O, Hatakeyama M, Saitoh H, Takada M. Different absorption behaviors among steroid hormones due to possible interaction with p-glycoprotein in the rat small intestine. *Biol Pharm Bull.* 1999;22(5):535–538. doi:10.1248/bpb.22.535.
- Cross TW, Kasahara K, Rey FE. Sexual dimorphism of cardiometabolic dysfunction: gut microbiome in the play? *Mol Metab.* 2018;15: 70–81. doi:10.1016/j.molmet.2018.05.016.
- Li D, Liu R, Wang M, Peng R, Fu S, Fu A, Le J, Yao Q, Yuan T, Chi H, and Mu X, et al. 3 β -hydroxysteroid dehydrogenase expressed by gut microbes degrades testosterone and is linked to depression in males. *Cell Host & Microbe.* 2022;30(1):e5. doi:10.1016/j.chom.2021.12.018.
- Sandberg AA, Wr S Jr. Metabolism of 4-C¹⁴-testosterone in human subjects. I. distribution in bile, blood, feces and urine. *J Clin Invest.* 1956;35(12):1331–1339. doi:10.1172/JCI103389.
- Neuman H, Debelius JW, Knight R, Koren O, Banin E. Microbial endocrinology: the interplay between the microbiota and the endocrine system. *FEMS Microbiol Rev.* 2015;39(4):509–521. doi:10.1093/femsre/fuu010.
- Vom Steeg LG, Klein SL. Sex steroids mediate bidirectional interactions between hosts and microbes. *Horm Behav.* 2017;88: 45–51. doi:10.1016/j.yhbeh.2016.10.016.

18. Koppel N, Balskus EP. Exploring and understanding the biochemical diversity of the human microbiota. *Cell Chem Biol.* 2016;23(1):18–30. doi:10.1016/j.chembiol.2015.12.008.
19. Pandey AK, Sassetti CM. Mycobacterial persistence requires the utilization of host cholesterol. *Proc Natl Acad Sci U S A.* 2008;105(11):4376–4380. doi:10.1073/pnas.0711159105.
20. Van der Geize R, Yam K, Heuser T, Wilbrink MH, Hara H, Anderton MC, Sim E, Dijkhuizen L, Davies JE, Mohn WW, et al. A gene cluster encoding cholesterol catabolism in a soil actinomycete provides insight into *Mycobacterium tuberculosis* survival in macrophages. *Proc Natl Acad Sci U S A.* 2007;104(6):1947–1952. doi:10.1073/pnas.0605728104.
21. Crowe AM, Workman SD, Watanabe N, Worrall LJ, Strynadka NCJ, Eltis LD. IpdAB, a virulence factor in mycobacterium tuberculosis, is a cholesterol ring-cleaving hydrolase. *Proc Natl Acad Sci U S A.* 2018;115(15):E3378–87. doi:10.1073/pnas.1717015115.
22. Ridlon JM. Conceptualizing the vertebrate sterolbiome. *Appl Environ Microbiol.* 2020;86(16). e00641-20. doi:10.1128/AEM.00641-20.
23. Chiang Y-R, Wei S-S, Wang P-H, P-H W, C-P Y. Microbial degradation of steroid sex hormones: implications for environmental and ecological studies. *Microb Biotechnol.* 2020;13(4):926–949. doi:10.1111/1751-7915.13504.
24. Bergstrand LH, Cardenas E, Holert J, Van Hamme JD, Mohn WW. Delineation of steroid-degrading microorganisms through comparative genomic analysis. *MBio.* 2016;7(4):e00166. doi:10.1128/mBio.00865-16.
25. Holert J, Cardenas E, Bergstrand LH, Zaikova E, Hahn AS, Hallam SJ, Mohn WW. Metagenomes reveal global distribution of bacterial steroid catabolism in natural, engineered, and host environments. *MBio.* 2018;9(1). e02345-17. doi:10.1128/mBio.02345-17.
26. Horinouchi M, Koshino H, Malon M, Hirota H, Hayashi T, Müller V. Steroid degradation in comamonas testosteroni TA441: identification of metabolites and the genes involved in the reactions necessary before D-ring cleavage. *Appl Environ Microbiol.* 2018;84(22). e01324-18. doi:10.1128/AEM.01324-18.
27. Dresen C, Lin L-C, D'angelo I, Tocheva EI, Strynadka N, Eltis LD. A flavin-dependent monooxygenase from mycobacterium tuberculosis involved in cholesterol catabolism. *J Biol Chem.* 2010;285(29):22264–22275. doi:10.1074/jbc.M109.099028.
28. Capyk JK, Casabon I, Gruninger R, Strynadka NC, Eltis LD. Activity of 3-ketosteroid 9 α -hydroxylase (KshAB) indicates cholesterol side chain and ring degradation occur simultaneously in mycobacterium tuberculosis. *J Biol Chem.* 2011;286(47):40717–40724. doi:10.1074/jbc.M111.289975.
29. Wang P-H, Leu Y-L, Ismail W, Tang S-L, Tsai C-Y, Chen H-J, Kao A-T, Chiang Y-R. Anaerobic and aerobic cleavage of the steroid core ring structure by steroidobacter denitrificans. *J Lipid Res.* 2013;54(5):1493–1504. doi:10.1194/jlr.M034223.
30. Yang F-C, Chen Y-L, Tang S-L, Yu C-P, Wang P-H, Ismail W, Wang C-H, Ding J-Y, Yang C-Y, Yang C-Y, et al. Integrated multi-omics analyses reveal the biochemical mechanisms and phylogenetic relevance of anaerobic androgen biodegradation in the environment. *Isme J.* 2016;10(8):1967–1983. doi:10.1038/ismej.2015.255.
31. Shih C-J, Chen Y-L, Wang C-H, Wei S-S, Lin I-T, Ismail WA, et al. Biochemical mechanisms and microorganisms involved in anaerobic testosterone metabolism in estuarine sediments. *Front Microbiol.* 2017;8:1520. doi:10.3389/fmicb.2017.01520.
32. Zhang B, Lv Z, Li Z, Wang W, Li G, Guo Y. Dietary l-arginine supplementation alleviates the intestinal injury and modulates the gut microbiota in broiler chickens challenged by clostridium perfringens. *Front Microbiol.* 2018;9:1716.
33. Li A, Wang Y, He Y, Liu B, Iqbal M, Mehmood K, Jamil, T., Chang, Y.F., Hu, L., Li, Y. and Guo, J., et al. Environmental fluoride exposure disrupts the intestinal structure and gut microbial composition in ducks. *Chemosphere.* 2021;277:130222. doi:10.1016/j.chemosphere.2021.130222.
34. Xu Y, Xie Z, Wang H, Shen Z, Guo Y, Gao Y, et al. Bacterial diversity of intestinal microbiota in patients with substance use disorders revealed by 16S rRNA gene deep sequencing. *Sci Rep.* 2017;7(1):3628. doi:10.1038/s41598-017-03706-9.
35. Cusotto S, Clarke G, Dinan TG, Cryan JF. Psychotropics and the microbiome: a chamber of secrets. . . . *Psychopharmacology.* 2019;236(5):1411–1432. doi:10.1007/s00213-019-5185-8.
36. Maini Rekdal V, Nol Bernadino P, Luescher MU, Kiamehr S, Le C, Bisanz JE, et al. A widely distributed metalloenzyme class enables gut microbial metabolism of host- and diet-derived catechols. *Elife.* 2020;9:e50845. doi:10.7554/eLife.50845.
37. Ley RE, Hamady M, Lozupone C, Turnbaugh PJ, Ramey RR, Bircher JS, Schlegel ML, Tucker TA, Schrenzel MD, Knight R, et al. Evolution of mammals and their gut microbes. *Science.* 2008;320(5883):1647–1651. doi:10.1126/science.1155725.
38. Leu Y-L, Wang P-H, Shiao M-S, Ismail W, Chiang Y-R. A novel testosterone catabolic pathway in bacteria. *J Bacteriol.* 2011;193(17):4447–4455. doi:10.1128/JB.00331-11.
39. Po-Hsiang W, Chang-Ping Y, Tzong-Huei L, Ching-Wen L, Wael I, Shiao-Pyng W, Kuo A-T, Chiang Y-R. Anoxic androgen degradation by the denitrifying bacterium *Sterolibacterium denitrificans* via the 2,3-seco pathway. *Appl Environ Microbiol.* 2014;80(11):3442–3452. doi:10.1128/AEM.03880-13.
40. Yam KC, D'angelo I, Kalscheuer R, Zhu H, Wang J-X, Snieckus V, Ly LH, Converse PJ, Jacobs WR, Strynadka N, et al. Studies of a ring-cleaving

- dioxygenase illuminate the role of cholesterol metabolism in the pathogenesis of mycobacterium tuberculosis. *PLoS Pathog.* 2009;5(3):e1000344. doi:10.1371/journal.ppat.1000344.
41. Capyk JK, D'angelo I, Strynadka NC, Eltis LD. Characterization of 3-ketosteroid 9 α -hydroxylase, a rieske oxygenase in the cholesterol degradation pathway of mycobacterium tuberculosis. *J Biol Chem.* 2009;284(15):9937–9946. doi:10.1074/jbc.M900719200.
 42. Livak KJ, Schmittgen TD. Analysis of relative gene expression data using real-time quantitative PCR and the 2^{- $\Delta\Delta$ CT} method. *Methods.* 2001;25: 402–408. doi:10.1006/meth.2001.1262.
 43. Matsushita M, Fujita K, Motooka D, Hatano K, Fukae S, Kawamura N, Tomiyama E, Hayashi Y, Banno E, Takao T, et al. The gut microbiota associated with high-Gleason prostate cancer. *Cancer Sci.* 2021;112(8):3125–3135. doi:10.1111/cas.14998.
 44. Anders HJ, Kaetzke A, Kämpfer P, Ludwig W, Fuchs G. Taxonomic position of aromatic-degrading denitrifying pseudomonad strains K 172 and KB 740 and their description as new members of the genera thauera, as thauera aromatica sp. nov., and azoarcus, as azoarcus evansii sp. nov., respectively, members of the beta subclass of the proteobacteria. *Int J Syst Bacteriol.* 1995;45(2):327–333. doi:10.1099/00207713-45-2-327.
 45. Foss S, Harder J. *Thauera linaloolentis* sp. nov. and thauera terpenica sp. nov., isolated on oxygen-containing monoterpenes (linalool, menthol, and eucalyptol) nitrate. *Syst Appl Microbiol.* 1998;21(3):365–373. doi:10.1016/S0723-2020(98)80046-5.
 46. Stokes NA, Hylemon PB. Characterization of and 3 β -hydroxysteroid dehydrogenase in cell extracts of *Clostridium innocuum*. *Biochim Biophys Acta.* 1985;836(2):255–261. doi:10.1016/0005-2760(85)90073-6.
 47. Booiijink CCGM, Boekhorst J, Zoetendal EG, Smidt H, Kleerebezem M, de Vos WM. Metatranscriptome analysis of the human fecal microbiota reveals subject-specific expression profiles, with genes encoding proteins involved in carbohydrate metabolism being dominantly expressed. *Appl Environ Microbiol.* 2010;76(16):5533–5540. doi:10.1128/AEM.00502-10.
 48. Waldbauer JR, Newman DK, Summons RE. Microaerobic steroid biosynthesis and the molecular fossil record of Archean life. *Proc Natl Acad Sci U S A.* 2011;108(33):13409–13414. doi:10.1073/pnas.1104160108.
 49. Singhal R, Shah YM. Oxygen battle in the gut: hypoxia and hypoxia-inducible factors in metabolic and inflammatory responses in the intestine. *J Biol Chem.* 2020;295(30):10493–10505. doi:10.1074/jbc.REV120.011188.
 50. Lin C-W, Wang P-H, Ismail W, Tsai Y-W, El Noyal A, Yang C-Y, Yang F-C, Wang C-H, Chiang Y-R. Substrate uptake and subcellular compartmentation of anoxic cholesterol catabolism in *Sterolibacterium denitrificans*. *J Biol Chem.* 2015;290(2):1155–1169. doi:10.1074/jbc.M114.603779.
 51. Mayneris-Perxachs J, Arnoriaga-Rodríguez M, Luque-Córdoba D, Priego-Capote F, Pérez-Brocal V, Moya A, Burokas A, Maldonado R, Fernández-Real J-M. Gut microbiota steroid sexual dimorphism and its impact on gonadal steroids: influences of obesity and menopausal status. *Microbiome.* 2020;8(1):136. doi:10.1186/s40168-020-00913-x.
 52. Doden HL, Pollet RM, Mythen SM, Wawrzak Z, Devendran S, Cann I, Koropatkin NM, Ridlon JM. Structural and biochemical characterization of 20 β -hydroxysteroid dehydrogenase from bifidobacterium adolescentis strain L2-32. *J Biol Chem.* 2019;294(32):12040–12053. doi:10.1074/jbc.RA119.009390.
 53. Huang P-Y, Yang Y-C, Wang C-I, Hsiao P-W, Chiang H-I, Chen T-W. Increase in akkermansiaceae in gut microbiota of prostate cancer-bearing mice. *Int J Mol Sci.* 2021;22(17):9626. doi:10.3390/ijms22179626.
 54. Pfennig N. *Rhodocyclus purpureus* gen. nov. and sp. nov., a ring-shaped, vitamin B12-requiring member of the family rhodospirillaceae. *Int J Syst Bacteriol.* 1980;30(1):224. doi:10.1099/00207713-30-1-224.
 55. Rabus R, Widdel F. Anaerobic degradation of ethylbenzene and other aromatic hydrocarbons by new denitrifying bacteria. *Arch Microbiol.* 1995;163(2):96–103. doi:10.1007/BF00381782.
 56. Tschsch A, Pfennig N. Growth yield increase linked to caffeate reduction in acetobacterium woodii. *Arch Microbiol.* 1984;137: 163–167. doi:10.1007/BF00414460.
 57. Kolmogorov M, Yuan J, Lin Y, Pevzner PA. Assembly of long, error-prone reads using repeat graphs. *Nat Biotechnol.* 2019;37(5):540–546. doi:10.1038/s41587-019-0072-8.
 58. Boetzer M, Pirovano W. SSPACE-LongRead: scaffolding bacterial draft genomes using long read sequence information. *BMC Bioinform.* 2014;15: 211. doi:10.1186/1471-2105-15-211.
 59. English AC, Richards S, Han Y, Wang M, Vee V, Qu J, Qin X, Muzny DM, Reid JG, Worley KC, et al. Mind the gap: upgrading genomes with pacific biosciences RS long-read sequencing technology. *PLoS One.* 2012;7(11):e47768. doi:10.1371/journal.pone.0047768.
 60. Hunt M, Silva ND, Otto TD, Parkhill J, Keane JA, Harris SR. Circlator: automated circularization of genome assemblies using long sequencing reads. *Genome Biol.* 2015;16(1):294. doi:10.1186/s13059-015-0849-0.
 61. Gurevich A, Saveliev V, Vyahhi N, Tesler G. QUAST: quality assessment tool for genome assemblies. *Bioinformatics.* 2013;29(8):1072–1075. doi:10.1093/bioinformatics/btt086.
 62. Seemann T. Prokka: rapid prokaryotic genome annotation. *Bioinformatics.* 2014;30(14):2068–2069. doi:10.1093/bioinformatics/btu153.

63. Farnsworth R, Keating J, McAuley M, Smith R. Optimization of a protocol for *Escherichia coli* RNA extraction and visualization. *J Exp Microbiol Immunol*. 2004;5:87–94.
64. Kleindienst S, Higgins SA, Tsementzi D, Chen G, Konstantinidis KT, Mack EE, Löffler FE. ‘*Candidatus dichloromethanomonas elyunquensis*’ gen. nov., sp. nov., a dichloromethane-degrading anaerobe of the peptococcaceae family. *Syst Appl Microbiol*. 2017;40(3):150–159. doi:10.1016/j.syapm.2016.12.001.
65. Kozich JJ, Westcott SL, Baxter NT, Highlander SK, Schloss PD. Development of a dual-index sequencing strategy and curation pipeline for analyzing amplicon sequence data on the MiSeq Illumina sequencing platform. *Appl Environ Microbiol*. 2013;79(17):5112–5120. doi:10.1128/AEM.01043-13.
66. Oksanen J, Blanchet FG, Kindt R, Legendre P, Minchin PR, O’hara R, Simpson GL, Solymos P, Stevens MHH, Wagner H. Package ‘vegan’. *Community Ecology Package, Version*. 2013;2:1–295.
67. Love MI, Huber W, Anders S. Moderated estimation of fold change and dispersion for RNA-seq data with DESeq2. *Genome Biol*. 2014;15(12):550. doi:10.1186/s13059-014-0550-8.
68. Metsalu T, Vilo J. ClustVis: a web tool for visualizing clustering of multivariate data using principal component analysis and heatmap. *Nucleic Acids Res Oxford Academic*. 2015;43(W1):W566–70. doi:10.1093/nar/gkv468.
69. Friedman J, Alm EJ, von Mering C. Inferring correlation networks from genomic survey data. *PLoS Comput Biol*. 2012;8(9):e1002687. doi:10.1371/journal.pcbi.1002687.
70. Kurtz ZD, Müller CL, Miraldi ER, Littman DR, Blaser MJ, Bonneau RA, von Mering C. Sparse and compositionally robust inference of microbial ecological networks. *PLoS Comput Biol*. 2015;11(5):e1004226. doi:10.1371/journal.pcbi.1004226.
71. Bastian M, Heymann S, Jacomy M. Gephi: an open source software for exploring and manipulating networks. *ICWSM*. 2009;3(1):361–362. doi:10.1609/icwsml.v3i1.13937.
72. Peschel S, Müller CL, von Mutius E, Boulesteix A-L, Depner M. NetCoMi: network construction and comparison for microbiome data in R. *Brief Bioinform*. 2021;22(4):bbaa290. doi:10.1093/bib/bbaa290.
73. Cameron LMG, Booth TJ, van Wersch B, van Grieken L, Medema MH, Yit-Heng Chooi, cblaster: a remote search tool for rapid identification and visualization of homologous gene clusters. *Bioinformatics Advances*. 2021;1(1). vbab016. doi:10.1093/bioadv/vbab016.
74. Bacchetti De Gregoris T, Aldred N, Clare AS, Burgess JG. Improvement of phylum- and class-specific primers for real-time PCR quantification of bacterial taxa. *J Microbiol Methods*. 2011;86(3):351–356. doi:10.1016/j.mimet.2011.06.010.
75. Herlemann DPR, Labrenz M, Jürgens K, Bertilsson S, Waniek JJ, Andersson AF. Transitions in bacterial communities along the 2000 km salinity gradient of the Baltic Sea. *Isme J*. 2011;5(10):1571–1579. doi:10.1038/ismej.2011.41.